Interaction of an Adsorbed Atom with a Laser

by

Henk F. Arnoldus, Sander van Smaalen and Thomas F. George

Prepared for Publication

in

Advances in Chemical Physics

Departments of Chemistry and Physics
State University of New York at Buffalo
Buffalo, New York 14260

December 1986

AD-A175 751

DTIC FILE COPY

JAN 6 1987

A

87   1   6   019

AD·A175751

REPORT DOCUMENTATION PAGE

1a. REPORT SECURITY CLASSIFICATION	1b. RESTRICTIVE MARKINGS
Unclassified	

2a. SECURITY CLASSIFICATION AUTHORITY	3. DISTRIBUTION/AVAILABILITY OF REPORT
	Approved for public release; distribution unlimited
2b. DECLASSIFICATION/DOWNGRADING SCHEDULE	

4. PERFORMING ORGANIZATION REPORT NUMBER(S)	5. MONITORING ORGANIZATION REPORT NUMBER(S)
UBUFFALO/DC/86/TR-23	

6a. NAME OF PERFORMING ORGANIZATION	6b. OFFICE SYMBOL (If applicable)	7a. NAME OF MONITORING ORGANIZATION
Depts. Chemistry & Physics State University of New York		

6c. ADDRESS (City, State and ZIP Code)	7b. ADDRESS (City, State and ZIP Code)
Fronczak Hall, Amherst Campus Buffalo, New York 14260	Chemistry Program 800 N. Quincy Street Arlington, Virginia 22217

8a. NAME OF FUNDING/SPONSORING ORGANIZATION	8b. OFFICE SYMBOL (If applicable)	9. PROCUREMENT INSTRUMENT IDENTIFICATION NUMBER
Office of Naval Research		Contract N00014-86-K-0043

8c. ADDRESS (City, State and ZIP Code)	10. SOURCE OF FUNDING NOS.			
Chemistry Program 800 N. Quincy Street Arlington, Virginia 22217	PROGRAM ELEMENT NO.	PROJECT NO.	TASK NO.	WORK UNIT NO.

11. TITLE
Interaction of an Adsorbed Atom with a Laser

12. PERSONAL AUTHOR(S)
Henk F. Arnoldus, Sander van Smaalen and Thomas F. George

13a. TYPE OF REPORT	13b. TIME COVERED	14. DATE OF REPORT (Yr., Mo., Day)	15. PAGE COUNT
	FROM _____ TO _____	December 1986	54

16. SUPPLEMENTARY NOTATION
Prepared for publication in Advances in Chemical Physics

17. COSATI CODES			18. SUBJECT TERMS (Continue on reverse if necessary and identify by block number)	
FIELD	GROUP	SUB. GR.	KINETIC PHONON COUPLING,	DRESSED STATES
			THERMAL RELAXATION,	LASER HEATING
			LINE SHAPE,	PHOTON-PHONON CONVERSION

19. ABSTRACT (Continue on reverse if necessary and identify by block number)

The irradiation by infrared laser light of an atom adsorbed on the surface of a harmonic crystal is considered. The dynamic coupling between the atom (its motion) and the substrate degrees of freedom (phonon field) in the presence of a confining potential well (van der Waals bond between atom and crystal) gives rise to thermal relaxation of this adbond configuration. Both the atom and the substrate are assumed to be transparent, but the bond is allowed to have non-vanishing dipole-moment matrix elements, which couple the external field to the adsorbate. The equation of motion for the reduced adbond density operator is obtained with reservoir theory, and the relaxation constants are expressed in properties of the crystal. With a similar method, the spectral profile for absorption of weak radiation is derived. Subsequently, the illumination by a strong finite-linewidth laser field which is in close resonance with a single transition of the adbond is examined. The optical Bloch equations in operator form are derived and applied to study the process of laser heating of the crystal. It is pointed out how this mechanism can be understood as resulting from (multi)photon-phonon conversion reactions which are mediated by the adbond.

20. DISTRIBUTION/AVAILABILITY OF ABSTRACT	21. ABSTRACT SECURITY CLASSIFICATION
UNCLASSIFIED/UNLIMITED ☒ SAME AS RPT. ☒ DTIC USERS ☐	Unclassified

22a. NAME OF RESPONSIBLE INDIVIDUAL	22b. TELEPHONE NUMBER (Include Area Code)	22c. OFFICE SYMBOL
Dr. David L. Nelson	(202) 696-4410	

DD FORM 1473, 83 APR   EDITION OF 1 JAN 73 IS OBSOLETE.

INTERACTION OF AN ADSORBED ATOM WITH A LASER

Henk F. Arnoldus, Sander van Smaalen and Thomas F. George
Departments of Physics & Astronomy and Chemistry
239 Fronczak Hall
State University of New York at Buffalo
Buffalo, New York 14260

CONTENTS

ABSTRACT

The irradiation by infrared laser light of an atom adsorbed on the surface of a harmonic crystal is considered. The dynamic coupling between the atom (its motion) and the substrate degrees of freedom (phonon field) in the presence of a confining potential well (van der Waals bond between atom and crystal) gives rise to thermal relaxation of this adbond configuration. Both the atom and the substrate are assumed to be transparent, but the bond is allowed to have non-vanishing dipole-moment matrix elements, which couple the external field to the adsorbate. The equation of motion for the reduced adbond density operator is obtained with reservoir theory, and the relaxation constants are expressed in properties of the crystal. With a similar method, the spectral profile for absorption of weak radiation is derived. Subsequently, the illumination by a strong finite-linewidth laser field which is in close resonance with a single transition of the adbond is examined. The optical Bloch equations in operator form are derived and applied to study the process of laser heating of the crystal. It is pointed out how this mechanism can be understood as resulting from (multi)photon-phonon conversion reactions which are mediated by the adbond.

I. INTRODUCTION

Applications of tunable laser sources in contemporary experiments in physics and chemistry ca. roughly be subdivided into two categories. In the first class the laser is used as a diagnostic tool to investigate a dynamical system with spectroscopic methods. Scanning the frequency of a low-power field which is incident on an atom or molecule reveals the resonances of the system as lines in the absorption profile. Interaction of the system with the environment (collisions, spontaneous emission, presence of boundaries, etc.) amounts to relaxation of the molecule, which in turn broadens a spectral line in such a way that the width of the line is proportional to the inverse relaxation rate of the specific transition. More subtle properties of the line shape, such as the far-wing decay, carry information on the details of the interaction, since the frequency dependence of the absorption is determined by the Fourier-Laplace transform of the time-evolution operator of the density operator.[1] Therefore, it can be expected that a profound comprehension of dynamical properties can be achieved from an accurate observation of spectral profiles. However, this method requires an elaborate theory which disentangles the contributions of the various mechanisms to the line shape.

In the second category of experiments, a radiation field is applied in order to modify or even induce a process. An incident photon can supply the necessary activation energy for a reaction which is very unlikely to take place without a field. The advantage of a narrow-band laser is that by tuning the laser frequency, the process can be optimized, in contrast to, for instance, thermal excitation of a species (collisions). Prime examples are laser-induced dissociation and ionization and atomic resonance fluorescence. In more rigorous situations, a strong (pulsed) laser is merely used as a heat gun (melting,

vaporization), and the color and polarization of the field are not of crucial importance.[2]

In the present paper we consider optical features of atoms which are adsorbed on a crystal. An atom is bounded to the substrate by electromagnetic interaction with the crystal atoms (van der Waals energy), which is effectively described by a potential well. The few (~25) vibrational adbond states have transition frequencies (level separations) of the order of 50 cm^{-1} up to 500 cm^{-1}, which is in the infrared (IR) region of the optical spectrum. Both the atom and the crystal are supposed to be transparent for IR light, as is for instance the case for noble-gas atoms on potassium chloride. The vibrational states, however, exhibit an optical activity in the sense that there are non-vanishing dipole matrix elements between the various bound states. Irradiation with an IR laser will then amount to photon absorption by the bond, and hence the spectral profile will reflect the properties of the binding potential and the dynamical interaction with the substrate. In this fashion we can study transparent crystals with spectroscopic methods, where the medium for transport of the information is furnished by the adsorbed atoms. This situation is reminiscent of the more familiar problem of collisional redistribution by neutrals in gas-phase experiments. Transparent atoms are immersed in a buffer gas, and photons from an incident field are absorbed during collisions only. Accurate measurements of line shapes then allow the determination of interaction potentials. The only distinction is that collisional redistribution deals with scattering states, whereas the spectroscopy of adsorbates involves bound states. It can be anticipated that the established methods for the gas phase can be converted into suitable surface equivalents, although experiments along this line are still rare.[3,4]

Efforts in the second category of the application of lasers in this system are far more common, and most notably studied is the process of resonant desorption.[5-7] An intense IR laser is tuned into resonance with the transition frequency between a low-lying and a high-lying vibrational state. Absorption of a photon is accompanied by a transition of the adbond to the high-lying state, which is close to the continuum. Then the crystal, regarded as a thermal bath, has only to provide a small amount of energy in order to accomplish the desorption of the atom. Without the driving laser this process would not occur, since the atomic bond has to be excited to the high-lying state by thermal coupling to the substrate. In this way, one has expected to be able to make clean surfaces, without heating (as in thermal desorption) or damaging the materials.[8-13] Another idea has been that advantage could be taken of the resonant nature of the process. Different adsorbed species would be desorbed selectively, depending on the laser frequency, which would provide a practical method for isotope separation, or less ambitious, separation of molecules.[12-13] Although the sketched process will obviously happen if the radiative coupling is sufficiently strong, it does not necessarily mean that the efficiency is very high. Recent experiments[8] show a quantum yield of about 1% (ratio of desorbed atoms to absorbed photons), which conversely implies that almost all radiation is converted into thermal energy of the substrate. Consequently, the solid heats up very fast, and this is precisely what one tries to avoid. Since the thermal coupling is inevitable, the conclusion is that resonant desorption is not a very promising technique. Furthermore, the selectivity has turned out to be very poor, if present at all, which is probably due to a rapid energy exchange between different adsorbates preceeding the desorption.[14] From a different point of view, however, this mechanism could be applied for laser heating of a transparent crystal. By manipulating the spatial variations of the

laser intensity, this process can be used to maintain well-controlled temperature gradients along a gas-solid interface.

II. KINETIC PHONON COUPLING

An atom with mass m is physisorbed on the surface (xy-plane) of a crystal, and its motion is assumed to be mainly perpendicular to the surface (z-direction). The interaction potential with the solid is subdivided into two parts, V_1 and V_2, where V_1 represents the potential well resulting from the coupling to the closest surface atom, and V_2 is an effective repulsive potential, which is brought about by the remainder of the crystal and confines the atom to the region $z > 0$. The thermal-equilibrium position of the nearest surface atom, with mass M, is taken as the origin of the coordinate system. Then the positions of m and M are denoted by $z\underline{e}_z$ and $\underline{u}$, respectively, and V_1 depends on $|z\underline{e}_z - \underline{u}|$ only, whereas V_2 depends on z. Subsequently, it can be asserted that $\underline{u}$ (~ 0.1 Å) is much smaller than z (> 1 Å), which allows a Taylor expansion of V_1 around $\underline{u} = 0$. Hence we can write

$$V_1(|z\underline{e}_z - \underline{u}|) = V_1(z) - \underline{u}\cdot\underline{e}_z \frac{dV_1}{dz} + \ldots \tag{2.1}$$

and then omit the ellipsis. In physical terms this means that we neglect multiphonon processes in comparison with single-phonon transitions, as will become clear in due course.

Next we notice that the expansion (2.1) separates the coupling with the lattice vibrations (last term) from the interaction $V_1(z)$ with the static crystal, which equals the interaction for $\underline{u} = 0$. A convenient basis set for the adbond wave function is therefore provided by the eigenstates of the adbond Hamiltonian H_a, defined as

$$H_a = - \frac{\hbar^2}{2m} \frac{d^2}{dz^2} + V_1(z) + V_2(z) \qquad (2.2)$$

where the first term is the kinetic energy. Once a potential is prescribed, the eigenvalues $\hbar\omega_i$ and the eigenfunctions $|i\rangle$ of the H_a can be evaluated with standard methods. A common choice for the combination $V_1(z) + V_2(z)$ is a Morse potential[15-19] or a truncated harmonic potential.[20] We shall not refer to a specific potential in this paper, but only use the eigenvalue equation

$$H_a|i\rangle = \hbar\omega_i|i\rangle \qquad (2.3)$$

and assume the eigenstates to be non-degenerate (as for a Morse potential). Then in turn we can represent H_a with respect to its own eigenstates as

$$H_a = \sum_i \hbar\omega_i P_i \qquad (2.4)$$

with $P_i = |i\rangle\langle i|$ the projector on the i-th adbond state.

As a model for the crystal we adopt a harmonic-lattice representation, for which the Hamiltonian reads[21]

$$H_p = \sum_{\underset{\sim}{k}s} \hbar\omega(k)a^\dagger_{\underset{\sim}{k}s}a_{\underset{\sim}{k}s} \qquad (2.5)$$

in terms of the annihilation and creation operators for phonons (bosons) in the mode $\underset{\sim}{k}s$. The summation runs over the wave vectors $\underset{\sim}{k}$ and branches s which are supported by the crystal, and the dispersion relation $\omega = \omega(k)$ is taken to be independent of s and of the direction of $\underset{\sim}{k}$. Coupling between the phonon field and the adbond is brought about by the position operator $\underset{\sim}{u}$ of M, which equals the displacement field at the origin. Explicitly,

$$\underset{\sim}{u} = \sum_{\underset{\sim}{k}s} \{\frac{\hbar v}{2MV\omega(k)}\}^{\frac{1}{2}} (a_{\underset{\sim}{k}s} + a^\dagger_{-\underset{\sim}{k}s}) \underset{\sim}{e}_{\underset{\sim}{k}s} \qquad (2.6)$$

in terms of the volume v of a unit cell and the quantization volume V.

Combining everything then gives for the Hamiltonian of the adbond plus crystal

$$H = H_a + H_p - RS \qquad (2.7)$$

with the abbreviations

$$R = \underset{\sim}{u} \cdot \underset{\sim}{e}_z \quad , \quad S = dV_1/dz \quad . \qquad (2.8)$$

It will appear in the next section that it is advantageous to work with a density-operator formalism, so the equation of motion is

$$i\hbar\frac{d\rho}{dt} = [H,\rho] \quad , \quad \rho^{\dagger} = \rho \quad , \quad \mathrm{Tr}\rho = 1 \quad . \qquad (2.9)$$

From Eq. (2.6) we see that the interaction between adbond and crystal, -RS, is linear in the creation and annihilation operators, which implies that -RS can only induce transitions between crystal states which differ by not more than one phonon. In other words, by retaining only the linear term in the expansion (2.1), we discard multiphonon processes, which can be justified as long as any set of two adbond states is resonantly coupled by a single-phonon process. Physically this implies that any level separation $|\omega_i - \omega_j|$ must be smaller than the cut-off frequency of the dispersion relation, which is the Debye frequency ω_D.

III. THERMAL RELAXATION

The full density operator $\rho(t)$ of a single atom and a large crystal has not much significance. Since we are interested in the dynamics of the adbond, we consider the reduced density operator $\rho_o(t)$, defined as

$$\rho_o(t) = \mathrm{Tr}_p\rho(t) \qquad (3.1)$$

where the trace runs over all phonon states. On the other hand, the crystal is regarded as a large reservoir at temperature T, for which the density matrix equals

$$\bar{\rho}_p = \exp(-\beta H_p)[Tr_p \exp(-\beta H_p)]^{-1} \qquad (3.2)$$

with $\beta = (kT)^{-1}$. Coupling between the adbond and the heat bath then gives rise to the thermal relaxation of $\rho_0(t)$, and eventually $\rho_0(t)$ reaches a steady state

$$\bar{\rho}_0 = \lim_{t \to \infty} \rho_0(t) \qquad (3.3)$$

in which the atomic bond and the crystal are in thermal equilibrium.

It is a standard procedure in relaxation theory to derive an equation for the reduced density operator $\rho_0(t)$. Both projection techniques[22] and a reservoir approach [23,24] yield the same result, provided that equivalent approximations are made.[25] Here we will briefly summarize the derivation of Ref. 24 and adopt a Liouville-operator notation, which will allow a concise formulation. A Liouvillian L is related to a Hamiltonian H according to

$$L\rho = \hbar^{-1}[H,\rho] \qquad (3.4)$$

which defines the action of L on an arbitrary operator ρ in Hilbert space. Then one regards ρ as a vector in Liouville space and L as a linear operator in that space.[26] Consequently, an N-dimensional Hilbert space generates an N^2-dimensional Liouville space. Matrix representations of Liouvillians can be constructed in the very same way as for operators in Hilbert space. A theorem that follows immediately from Eq. (3.4) is

$$\exp(Ls)\rho = \exp(Hs/\hbar)\rho\exp(-Hs/\hbar) \qquad (3.5)$$

where, for instance, s = it.

Reservoir theory starts with a transformation of the equation of motion (2.9) to the interaction picture, where the coupling -RS is considered as the interaction. With

$$\hat{\rho}(t) = \exp[i(L_a + L_p)t]\rho(t) \tag{3.6}$$

Eq. (2.9) can be written as

$$i\hbar \frac{d}{dt} \hat{\rho}(t) = -W(t)\hat{\rho}(t) \tag{3.7}$$

where $W(t)$ is defined as the Liouvillian

$$W(t)\rho = [(\exp(i(L_a + L_p)t)(RS)),\rho] \tag{3.8}$$

for an arbitrary ρ. As the initial condition we choose

$$\rho(0) = \rho_o(0)\bar{\rho}_p \quad . \tag{3.9}$$

Then the identity

$$Tr_p(W(t)\rho(0)) = 0 \tag{3.10}$$

follows from the fact that $\bar{\rho}_p$ commutes with H_p, and from the explicit form of R, Eqs. (2.6) and (2.8), which gives $Tr_p R\bar{\rho}_p = 0$. If we now integrate Eq. (3.7), take the trace over the phonon states, and use Eq. (3.10), we find

$$\frac{d}{dt} \hat{\rho}_o(t) = -\hbar^{-2} Tr_p \int_0^t d\tau \, W(t)W(t-\tau)\hat{\rho}(t-\tau) \tag{3.11}$$

which is an exact integral of the equation of motion.

Obviously, the integral in Eq. (3.11) is awkward, and a series of approximations has to be made in order to obtain a manageable expression. The crucial step which has to be made is the factorization

$$\hat{\rho}(t-\tau) \doteq \hat{\rho}_o(t-\tau)\bar{\rho}_p \tag{3.12}$$

in the integrand of Eq. (3.11). Then we substitute the explicit form of $W(t)$, use Eq. (3.5) several times, and transform back to the Schrödinger picture with the inverse relation of Eq. (3.6). Finally we obtain

$$i \frac{d}{dt} \rho_o(t) = L_a \rho_o(t) - \frac{i}{2\pi} L_S \int_0^t d\tau \, \exp(iL_a\tau) L_c(\tau) \rho_o(t-\tau) \qquad (3.13)$$

where L_S and $L_c(\tau)$ are defined by

$$L_S \rho = [S, \rho]$$

$$L_c(\tau)\rho = G(\tau) S\rho - G(\tau)^* \rho S \qquad (3.14)$$

which involves the reservoir correlation function

$$G(\tau) = 2\pi \hbar^{-2} Tr_p R \bar{\rho}_p \exp(iL_p\tau) R \quad . \qquad (3.15)$$

Inspection of Eq. (3.13) shows that the coupling to the crystal only enters through the function $G(\tau)$. Approximation (3.12) is sufficient to separate reservoir and adbond operators, and the presence of the solid can be accounted for by a single function $G(\tau)$.

Of paramount importance for the validity of a reservoir approach is that $G(\tau)$ decays to zero (for $\tau \to \infty$) sufficiently quickly. Due to the interference between the many phonon modes, the typical decay time will be of the order of the inverse cut-off frequency of the spectrum, which is ω_D for a crystal. This will become more clear in the next section. Then $L_c(\tau)$ deviates from zero only for $\tau \doteq 0$, and the most crude approximation would be to replace it by an operator which is proportional to a delta function. It is easy, however, to do much better. The net effect of the coupling of the adbond to the crystal is a damping on a time scale which equals the inverse linewidth. Since this is very slow in comparison with ω_D^{-1}, we conclude that in the interaction picture, $\hat{\rho}(t-\tau)$

varies negligibly on a time scale ω_D^{-1}, and therefore we can replace $\hat{\rho}(t-\tau)$ by $\hat{\rho}(t)$ in Eq. (3.11). This is the Markov approximation, and the equivalent in the Schrödinger picture reads

$$\rho_o(t-\tau) \; \cong \; \exp(iL_a\tau)\rho_o(t) \qquad (3.16)$$

which can be inserted into Eq. (3.13). Then we can replace the upper integration limit by infinity, which yields for the equation of motion

$$i\frac{d}{dt}\,\rho_o(t) = (L_a - i\Gamma)\rho_o(t) \quad . \qquad (3.17)$$

Relaxation of the adbond due to the coupling to the phonon reservoir is now completely accounted for by the time-independent Liouvillian

$$\Gamma = \frac{1}{2\pi}\,L_s\int_0^\infty d\tau\;\exp(-iL_a\tau)L_c(\tau)\exp(iL_a\tau) \quad . \qquad (3.18)$$

An expansion of Γ in matrix elements with respect to adbond states will be given in Section V.

If we insert the expression for L_S and $L_c(\tau)$ in Eq. (3.18), and use relation (3.5) for the exponentials, then we find that Γ can alternatively be cast in the form

$$\Gamma\rho = L_S(Q\rho - \rho Q^\dagger) \qquad (3.19)$$

where the Hilbert-space operator Q is defined as

$$Q = \frac{1}{2\pi}\int_0^\infty d\tau\;G(\tau)\exp(-iL_a\tau)S \quad . \qquad (3.20)$$

The advantage is that Q only involves a single exponential. Furthermore, we directly find from the representation (3.19)

$$\mathrm{Tr}_a(\Gamma\rho) = 0 \quad , \quad (\Gamma\rho)^\dagger = \Gamma\rho^\dagger \qquad (3.21)$$

which guarantees the conservation of trace and Hermiticity in the time evolution of $\rho_o(t)$.

IV. RESERVOIR CORRELATION FUNCTION

Properties of the crystal which affect the time evolution of the adbond are all embodied in the correlation function $G(\tau)$. In order to illustrate quantitatively the behavior of $G(\tau)$, we adopt a simple Debye model, which will already reveal the most salient features of a crystal correlation function. In this model, the dispersion relation is taken to be

$$\omega(k) = ckH(\omega_D - ck) \tag{4.1}$$

with c the speed of sound and H the unit-step function. The expression (3.15) is easily evaluated with standard techniques.[23] It is elucidating to subdivide $G(\tau)$ in a spontaneous and a stimulated part, according to

$$G(\tau) = G(\tau)_{sp} + G(\tau)_{st} \tag{4.2}$$

where $G(\tau)_{sp}$ is by definition $G(\tau)$ for $T = 0$. Hence $G(\tau)_{sp}$ is independent of T and accounts for relaxation of the adbond due to the presence of the crystal, irrespective of its temperature. We find for this spontaneous part

$$G(\tau)_{sp} = \zeta\omega_D^{-1} \frac{(1 + i\omega_D\tau)\exp(-i\omega_D\tau) - 1}{(\omega_D\tau)^2} \tag{4.3}$$

with the parameter ζ given by

$$\zeta = 3\pi/\hbar M \quad. \tag{4.4}$$

The real and imaginary part of $G(\tau)_{sp}$ are plotted in Fig. 1. For the stimulated contribution we obtain

$$G(\tau)_{st} = 2\zeta\omega_D^{-3} \int_0^{\omega_D} d\omega \; n(\omega)\omega\cos(\omega\tau) \qquad (4.5)$$

which is plotted in Fig. 2 for two values of the temperature. Here $n(\omega)$ is the average number of phonons in mode ω, which is explicitly

$$n(\omega) = [\exp(\beta\hbar\omega) - 1]^{-1} \; . \qquad (4.6)$$

Figs. 1 and 2 illustrate that $G(\tau)$ tends to zero indeed on a time scale ω_D^{-1}, although the decay is not exponential.

From Eq. (3.20) it follows that the relaxation constants (matrix elements of Γ) are determined by the Fourier-Laplace transform of $G(\tau)$

$$\tilde{G}(\omega) = \frac{1}{\pi} \int_0^\infty d\tau \; \exp(i\omega\tau)G(\tau) \qquad (4.7)$$

with ω equal to a transition frequency $\omega_i - \omega_j$. From Eqs. (4.3) and (4.5) we readily derive

$$\tilde{G}(\omega)_{sp} = \zeta\omega_D^{-3}\omega H(\omega)H(\omega_D-\omega) - i\pi^{-1}\zeta\omega_D^{-3}(\omega_D + \omega\log|1-\omega_D/\omega|) \qquad (4.8)$$

$$\tilde{G}(\omega)_{st} = \zeta\omega_D^{-3}|\omega|n(|\omega|)H(\omega_D - |\omega|)$$

$$+ i\pi^{-1}\zeta\omega_D^{-3}P \int_0^{\omega_D} d\omega' \; n(\omega') \frac{2\omega\omega'}{\omega^2 - \omega'^2} \qquad (4.9)$$

where P stands for principal value. These functions are plotted in Figs. 3 and 4. For negative values of ω the real part of $\tilde{G}(\omega)_{sp}$ vanishes identically, which implies that this contribution to Γ represents a decaying part. The thermal part obeys the relation

$$\tilde{G}(-\omega)_{st} = \tilde{G}(\omega)_{st}^* \qquad (4.10)$$

which indicates that upward and downward transitions between two levels, due to the finite temperature of the crystal, have the same rate constant. Hence the genuine thermal-equilibrium distribution is brought about by the spontaneous part of the relaxation operator, which is temperature independent.

Setting ω equal to zero yields immediately

$$\int_0^\infty d\tau G(\tau) = \zeta \omega_D^{-2}(-1 + \pi kT/\hbar\omega_D) \tag{4.11}$$

which can be regarded as a measure of the strength of $G(\tau)$. For $kT \gtrsim \hbar\omega_D$ the stimulated transitions tend to dominate the spontaneous decay.

V. MATRIX ELEMENTS

Solving the equation of motion (3.17) for a particular configuration of adbond states requires an expansion in matrix elements. Taking the k, ℓ-th matrix element gives

$$\frac{d}{dt} \langle k|\rho_o(t)|\ell\rangle = -i\langle k|(L_a\rho_o(t))|\ell\rangle - \langle k|(\Gamma\rho_o(t))|\ell\rangle \quad . \tag{5.1}$$

It remains to express the right-hand side in matrix elements of $\rho_o(t)$. From the definition (3.4) of L_a and the expression (2.4) of H_a, we easily find for the first term

$$\langle k|(L_a\rho)|\ell\rangle = \Delta_{k\ell}\langle k|\rho|\ell\rangle \tag{5.2}$$

for an arbitrary ρ, where

$$\Delta_{k\ell} = \omega_k - \omega_\ell \tag{5.3}$$

is the level separation between the adbond states $|k\rangle$ and $|\ell\rangle$.

Slightly more complicated is the evaluation of the relaxation operator Γ. First we notice that the exponential in Eq. (3.20) can be expanded as

$$\exp(-iL_a\tau)\rho = \sum_{k\ell} \exp(-i\Delta_{k\ell}\tau)P_k\rho P_\ell \qquad (5.4)$$

which yields the representation for Q

$$Q = \frac{1}{2}\sum_{k\ell} \tilde{G}(\Delta_{\ell k})P_k S P_\ell \qquad (5.5)$$

in terms of the Fourier-Laplace transform of the correlation function. Then we insert Eq. (5.5) into Eq. (3.19) and use the closure relation

$$\sum_i P_i = 1 \qquad (5.6)$$

which finally gives

$$\langle k|(\Gamma\rho)|\ell\rangle = \frac{1}{2}\sum_{mn} (c_{kmmn}\langle n|\rho|\ell\rangle + c^*_{\ell mmn}\langle k|\rho|n\rangle)$$

$$- \frac{1}{2}\sum_{mn} (c_{n\ell km} + c^*_{mk\ell n})\langle m|\rho|n\rangle \qquad (5.7)$$

in terms of the parameters

$$c_{k\ell mn} = \langle k|S|\ell\rangle\langle m|S|n\rangle\tilde{G}(\Delta_{nm}) \quad . \qquad (5.8)$$

Equation (5.7) expresses the relaxation operator Γ in matrix elements of the derivative of the potential, $S = dV_1/dz$, and $\tilde{G}(\omega)$, evaluated at the frequencies $\Delta_{k\ell}$. The combination of Eqs. (5.1), (5.2) and (5.7) turns the equation of motion into a simple set of linear first-order differential equations, which can be solved directly once a potential and an initial state $\rho_0(0)$ are specified.

VI. ABSORPTION SPECTRUM

A density operator is not directly amenable to observation in an experiment. One way of measuring properties of an adsorbed atom is by probing

the system with a weak monochromatic laser. A field with intensity I_L (energy per unit of time that passes through a unit area, perpendicular to the direction of propagation) and polarization $\underset{\sim}{\varepsilon}_L$ is scanned over the resonances of the system, and the power absorption $I(\omega_L)$ (absorbed energy per unit of time) is measured as a function of the laser frequency ω_L. Photons are absorbed from the field by the joint system of atom, crystal and their interaction (although the atom and the crystal separately are both assumed to be transparent), so that the absorption profile exhibits the details of the coupling between the adbond and the phonon field, rather than the properties of the adsorbed atom (the potential) alone.

The interaction between the adsorbate and the radiation field is established by a dipole coupling. Since the motion of the atom is restricted to the z-direction, the dipole-moment operator $\underset{\sim}{\mu}$ can be written as $\mu \underset{\sim}{e}_z$, with μ an operator in the Hilbert space spanned by the eigenstates $|k\rangle$ of the adbond Hamiltonian H_a. With $\underset{\sim}{E}$ the electric component of the radiation field, we can include the interaction in the equation of motion (2.9) with the substitution

$$H \rightarrow H - \mu \underset{\sim}{e}_z \cdot \underset{\sim}{E} \quad . \tag{6.1}$$

The probe beam is considered to be very weak, so that we can compute the power absorption with the Golden Rule. From the Appendix of Ref. 1 we copy the formal result

$$I(\omega_L) = I_L \omega_L (\varepsilon_0 \hbar c')^{-1} |\underset{\sim}{e}_z \cdot \underset{\sim}{\varepsilon}_L|^2 \mathrm{Re} \int_0^\infty d\tau \, \exp(i\omega_L \tau) \mathrm{Tr}\bar{\rho}[\mu(\tau),\mu] \tag{6.2}$$

where c' is the speed of light and $\bar{\rho}$ is the thermal-equilibrium density operator of the entire system, but without the interaction $-\underset{\sim}{\mu}\cdot\underset{\sim}{E}$. The τ-dependence of

$\mu(\tau)$ is given by $\mu(\tau) = \exp(iL\tau)\mu$. We remark that the commutator gives rise to two terms, where $\mu(\tau)\mu$ $(\mu\mu(\tau))$ represents stimulated photon absorption (emission). The net absorption is the balance between the loss and gain term for photons in the laser mode.

Evaluation of expression (6.2) starts with the identity

$$\text{Tr}\bar{\rho}[\mu(\tau),\mu] = \text{Tr}\mu\exp(-iL\tau)[\mu,\bar{\rho}] \quad . \tag{6.3}$$

Then we introduce the quantity

$$D(\tau) = \exp(-iL\tau)[\mu,\bar{\rho}] \tag{6.4}$$

which is an operator in the entire phonon and adbond Hilbert space. With $D_o(\tau) = \text{Tr}_p D(\tau)$, the adbond part of $D(\tau)$, we can write Eq. (6.3) as

$$\text{Tr}\bar{\rho}[\mu(\tau),\mu] = \text{Tr}_a \mu D_o(\tau) \quad . \tag{6.5}$$

Then we notice that $D(\tau)$ obeys the differential equation

$$i\frac{d}{dt}D(\tau) = LD(\tau) \tag{6.6}$$

with initial condition

$$D(0) = [\mu,\bar{\rho}_o]\bar{\rho}_p \tag{6.7}$$

where we have assumed that $\bar{\rho} = \bar{\rho}_o\bar{\rho}_p$. The equation of motion (6.6) is identical to Eq. (2.9), which is sometimes referred to as the quantum-regression theorem.[27] This implies that the time regression of the dipole correlation function $D(\tau)$ is identical to the time evolution of the density operator $\rho(t)$. This, in turn, is tantamount to the statement that the dynamical properties of the system are reflected in the frequency dependence of the absorption profile, which elucidates the significance of a measurement of $I(\omega_L)$.

From Eq. (6.5) we see that we only have to solve Eq. (6.6) for the reduced correlation function $D_o(\tau)$, which can be done along the very same lines that led to Eq. (3.17). Hence we can immediately write down the solution, which is

$$D_o(\tau) = \exp(-i(L_a - i\Gamma)\tau)[\mu, \bar{\rho}_o] \quad . \tag{6.8}$$

Substitution into Eq. (6.2) and performing the τ integration then yields

$$I(\omega_L) = I_L \omega_L (\epsilon_0 \hbar c')^{-1} |\underset{\sim}{e}_z \cdot \underset{\sim}{\epsilon}_L|^2 \mathrm{Re}\mathrm{Tr}_a \mu \frac{i}{\omega_L - L_a + i\Gamma}[\mu, \bar{\rho}_o] \tag{6.9}$$

in terms of the steady-state solution $\bar{\rho}_o$ from Eq. (3.17), which obeys

$$(L_a - i\Gamma)\bar{\rho}_o = 0 \quad , \quad \mathrm{Tr}_a \bar{\rho}_o = 1 \quad , \quad \bar{\rho}_o^{\dagger} = \bar{\rho}_o \quad . \tag{6.10}$$

From conservation of trace in the time evolution of $\rho_o(t)$, it follows that

$$\lim_{\tau \to \infty} D_o(\tau) = \bar{\rho}_o \mathrm{Tr}_a[\mu, \bar{\rho}_o] = 0 \tag{6.11}$$

which proves that the principal part in the upper integration limit $\tau = \infty$ vanishes. Equation (6.10) is easily solved for any level configuration. Then we insert $\bar{\rho}_o$ into Eq. (6.9), which determines the absorption profile in terms of a matrix inversion.

VII. LINE SHAPE

Expression (6.9) represents the complete absorption profile as a function of ω_L. In order to disentangle the contributions from the various adbond resonances, we consider the situation of two levels $|1\rangle$ and $|2\rangle$ with separation $\omega_2 - \omega_1 = \omega_o > 0$, and we scan the laser over this resonance. The resulting profile $I(\omega_L)$ is then termed the line shape of this particular transition. With the expansion in matrix elements from Section V, we can write down immediately the equation of motion as a linear set of differential equations. With $\rho_{12} = \langle 1|\rho_o|2\rangle$ and so forth for the other ρ_{ij}, we btain

$$i \frac{d}{dt} \rho_{22} = -ia_{21}\rho_{22} + ia_{12}\rho_{11} \tag{7.1}$$

$$i \frac{d}{dt} \rho_{11} = ia_{21}\rho_{22} - ia_{12}\rho_{11} \tag{7.2}$$

$$i \frac{d}{dt} \rho_{21} = (\omega_o - i\eta)\rho_{21} + i\eta^* \exp(2i\psi_S)\rho_{12} \tag{7.3}$$

$$i \frac{d}{dt} \rho_{12} = i\eta \exp(-2i\psi_S)\rho_{21} - (\omega_o + i\eta^*)\rho_{12} \tag{7.4}$$

where we introduced the abbreviations for the relaxation parameters

$$a_{k\ell} = |\langle k|S|\ell\rangle|^2 \text{Re}\tilde{G}(\Delta_{k\ell}) \tag{7.5}$$

$$\eta = \tfrac{1}{2}|\langle 2|S|1\rangle|^2 (\tilde{G}(\omega_o) + \tilde{G}(-\omega_o)^*) \tag{7.6}$$

and neglected the couplings due to the small diagonal matrix elements $\langle 1|S|1\rangle$ and $\langle 2|S|2\rangle$. Furthermore, the phase ψ_S of $\langle 2|S|1\rangle$ is defined by

$$\langle 2|S|1\rangle = |\langle 2|S|1\rangle|\exp(i\psi_S) \quad . \tag{7.7}$$

Of course, we can choose the phase between $|1\rangle$ and $|2\rangle$ in such a way that $\psi_S = 0$, but it will turn out to be advantageous to postpone the definition of the relative phase.

The steady-state solution of the set (7.1) - (7.4) is readily found to be

$$\bar{n}_2 = a_{21}/(a_{21} + a_{12}) \quad , \quad \bar{n}_1 = a_{12}/(a_{21} + a_{12}) \tag{7.8}$$

for the populations $\bar{n}_k = \bar{\rho}_{kk}$, whereas the coherences $\bar{\rho}_{12}$ and $\bar{\rho}_{21}$ vanish. From the set (7.1) - (7.4) we read off the matrix representation

$$\omega_L - L_a + i\Gamma = \begin{pmatrix} \omega_L + ia_{21} & -ia_{12} & 0 & 0 \\ -ia_{21} & \omega_L + ia_{12} & 0 & 0 \\ 0 & 0 & \omega_L - \omega_0 + i\eta & -i\eta^* \exp(2i\psi_s) \\ 0 & 0 & -i\eta\exp(-2i\psi_s) & \omega_L + \omega_0 + i\eta^* \end{pmatrix} \tag{7.9}$$

on the basis $|2><2|$, $|1><1|$, $|2><1|$, $|1><2|$. The inverse of this matrix is then substituted into Eq. (6.9). Matrix elements of the dipole-moment operator are not necessarily real. We write

$$<2|\mu|1> = |<2|\mu|1>|\exp(i\psi_\mu) \tag{7.10}$$

and now we choose the phase of the wave function $|1>$ in such a way that $\psi_\mu = \psi_s$. Combining everything then gives for the absorption line

$$I(\omega_L) = I_L B(\bar{n}_1 - \bar{n}_2)\hbar\omega_L \frac{1}{\pi} \frac{4\omega_o \omega_L \text{Re}_\eta}{(\omega_o^2 - \omega_L^2 + 2\omega_o\text{Im}\eta)^2 + 4\omega_L^2(\text{Re}\eta)^2} \tag{7.11}$$

where the Einstein coefficient B for stimulated transitions between $|1>$ and $|2>$ is defined as

$$B = \pi(\varepsilon_o\hbar^2c')^{-1}|<2|\mu|1>\underline{e}_z \cdot \underline{\varepsilon}_L|^2 \quad . \tag{7.12}$$

Due to the fact the $\text{Re}\eta$ and $\text{Im}\eta$ are not necessarily small in comparison with ω_o, the line is not a simple Lorentzian. A few examples of $I(\omega_L)$ are drawn in Figs. 5 and 6.

VIII. SECULAR APPROXIMATION

A great simplification arises if the relaxation constants $c_{k\ell mn}$ are small in comparison with the transition frequencies $\Delta_{k\ell}$ of the free evolution of the adbond. In spectral terms this means that the widths and shifts of lines are small in comparison with their central frequency, so $|\eta| << \omega_o$ in the notation of the previous section. Then the Liouvillian L_a will dominate the time evolution of $\rho_o(t)$ in Eq. (3.17), and the coupling between eigenvectors of L_a with different eigenvalues can be neglected. Every frequency $\Delta_{k\ell}$ gives rise to a single line, and the time regression of the correlation function does not couple anymore between different lines. In this approximation, every line evolves in a

secular fashion, which explains the origin of the name "secular" for this limiting approximation.

Mathematically this implies that we can decouple the time evolution of the coherences $\langle k|\rho_0(t)|\ell\rangle$, $k \neq \ell$, from the equation for the populations $n_k(t) = \langle k|\rho_0(t)|k\rangle$, since the free evolution of $\langle k|\rho_0(t)|\ell\rangle$ is proportional to $\exp(-i\Delta_{k\ell}t)$, whereas $n_k(t)$ evolves with eigenvalue zero ($\Delta_{kk} = 0$). From the matrix representation of section V it then follows that the coherences decay exponentially to zero, and that the time evolution of the populations is governed by the master equation

$$\frac{d}{dt} n_k = \sum_\ell (n_\ell a_{\ell k} - n_k a_{k\ell}) \qquad (8.1)$$

where only the relaxation constants $a_{k\ell}$ from Eq. (7.5) appear. Equation (8.1) is a simple gain-loss balance for the population of level $|k\rangle$, and we can interpret the term $n_\ell a_{\ell k}$ as the rate of transitions from $|\ell\rangle$ to $|k\rangle$, due to single-phonon emission into the crystal ($\omega_\ell > \omega_k$), or energy absorption from the solid ($\omega_\ell < \omega_k$). The set of differential equations (8.1) should be accompanied by the constraint

$$\sum_k n_k = 1 \qquad (8.2)$$

which expresses conservation of trace.

From Eq. (8.1) it follows that the decay constant for level $|k\rangle$ can be written as

$$A_k = \sum_\ell a_{k\ell} \qquad (8.3)$$

which turns the master equation into

$$\frac{d}{dt} n_k = -A_k n_k + \sum_\ell n_\ell a_{\ell k} \quad . \tag{8.4}$$

We notice that in the secular limit, the relaxation constants, which determine the level populations, are real. The coherences, however, still acquire contributions from the imaginary parts of the $c_{k\ell mn}$'s, which amounts to the line shifts. An advantage of the secular limit is that the imaginary parts can be accounted for by attributing an effective level shift to each frequency ω_k, according to

$$\bar{\omega}_k = \omega_k + \frac{1}{2} \sum_\ell \mathrm{Imc}_{k\ell\ell k} \quad . \tag{8.5}$$

Then we consider this transformation done, and suppress the tilde henceforth. For further use, we remark that in the secular limit the relaxation operator can be expressed entirely in projection operators. We obtain

$$\Gamma\rho = \frac{1}{2} \sum_{k\ell} a_{k\ell} (P_k \rho + \rho P_k - 2 P_\ell \mathrm{Tr}_a P_k \rho) \tag{8.6}$$

as can be checked by inspection.

Obviously, the secular approximation is not suitable for the evaluation of the details of a line shape, since it turns every line into a Lorentzian. In the remainder of this paper we shall consider the effect of irradiation with a strong laser. Then the dominant features of this system will be determined by the driving field, rather than by the minor details of the coupling to the phonon field. Hence we can adopt the representation (8.6) for the relaxation operator from here on.

IX. COHERENT EXCITATION

Probing the adsorbate with a weak laser does not alter the dynamics of the system. In a different application of lasers in these configurations, one

deliberately tries to modify or affect the behavior of the system by driving a particular transition with a strong, resonant field. The coherent nature of a laser field (well-defined phase in its time evolution) provides essentially a different excitation mechanism than a coupling to a thermal bath, like the phonon reservoir. Along with the fact that the laser power can be very high, this then opens the possibility to drive the system away from thermal equilibrium. The presence of the radiation will tend to maintain a certain distribution of the population over the different levels, which has to compete with the thermal relaxation. Therefore, it can be anticipated that it should be feasible to actually change the dynamics of the adbond if the laser is sufficiently intense. As mentioned in the Introduction, the first goal has been to enhance the desorption by resonant excitation of the adbond.

Radiative transitions between vibrational adsorbate states have been studied extensively, both in the weak-field case[28-32] and for strong fields.[6,33-35] In the present paper we summarize and extend our own approach,[36-38] which is valid for arbitrary laser power and includes the effect of the laser linewidth. We shall again work with a Liouville notation, which allows a concise formulation. Suppose that the laser frequency is in close resonance with a single transition of the adbond only, and that it couples a ground state $|g\rangle$ (not necessarily the lowest state of the adbond) with an excited state $|e\rangle$, which are separated by

$$\omega_o = \omega_e - \omega_g > 0 \ . \qquad (9.1)$$

The idea is that $|e\rangle$ is one of the high-lying states in the potential well, which is very unlikely to be populated by thermal excitation. Then this configuration automatically excludes resonant coupling between other levels.

Radiative transitions only occur between $|e\rangle$ and $|g\rangle$, but the thermal coupling remains present between all levels.

The electric component of the laser field at the position of the adbond is given by

$$\underline{E}(t) = E_o \ \text{Re} \ \underline{\varepsilon}_L \exp\{-i[\omega_L t + \phi(t)]\} \qquad (9.2)$$

where $\phi(t)$ is a real-valued stochastic process, which is responsible for the broadening of the laser line around its central frequency ω_L. It can be shown[39] that the response of the system is quite insensitive for the stochastic details of $\phi(t)$, provided that we restrict the description to single-mode fields. We shall take $\phi(t)$ as the independent-increment process,[40] which covers the more familiar Gaussian white-noise and random-jump processes as special cases. The multiplicative stochastic differential equation for this diffusion process has been solved in the Appendix of Ref. 41, where it turns out that the spectral profile of the laser is a Lorentzian, whose half-width at half-maximum is denoted by λ.

The dipole coupling between the adbond and the laser field, Eq. (6.1), now attains the explicit form

$$-\underline{\mu} \cdot \underline{E}(t) = -\tfrac{1}{2}\hbar\Omega|e\rangle\langle g| \exp\{-i[\omega_L t + \phi(t)]\} + \text{Hermitian conjugate} \qquad (9.3)$$

where the usual rotating-wave approximation[42] has been made, and permanent dipole-moments have been omitted. The strength of the coupling is determined by the Rabi frequency

$$\Omega = \hbar^{-1} E_o |\langle e|\underline{\mu} \cdot \underline{\varepsilon}_L|g\rangle| \quad . \qquad (9.4)$$

Then the equation of motion for the reduced density operator becomes

$$i\hbar\frac{d}{dt}\rho_o(t) = [H_a - \underline{\mu}\cdot\underline{E}(t),\rho_o(t)] - i\hbar\Gamma\rho_o(t) \tag{9.5}$$

which now contains the interaction with the external field explicitly.

A convenient way to eliminate the fast oscillations with the optical frequency ω_L from the Hamiltonian is by the introduction of the stochastic unitary transformation[43]

$$\sigma(t) = \exp\{-i[\omega_L t + \phi(t)]L_g\}\rho_o(t) \tag{9.6}$$

which contains the Liouvillian

$$L_g\rho = [P_g,\rho] \quad . \tag{9.7}$$

It is easy to check that the transformation only affects the coherences, so that we have

$$\langle k|\sigma(t)|k\rangle = n_k(t) \tag{9.8}$$

for every level $|k\rangle$. With some algebra, we find the transformed equation of motion to be

$$i\frac{d}{dt}\sigma(t) = (L_d + \dot{\phi}(t)L_g - i\Gamma)\sigma(t) \tag{9.9}$$

with $L_d\rho = \hbar^{-1}[H_d,\rho]$ and

$$H_d = H_a + \hbar\omega_L P_g - \tfrac{1}{2}\hbar\Omega(|e\rangle\langle g| + |g\rangle\langle e|) \tag{9.10}$$

the dressed-adbond Hamiltonian. This H_d has the significance of representing the free adbond (H_a), the free evolution of the single laser-mode and their dipole coupling. Phonon transitions (Γ) and phase fluctuations ($\dot{\phi}(t)L_g$) couple the eigenstates of H_d, which both give rise to relaxation of $\sigma(t)$.

The appearance of the time derivative $\dot{\phi}(t)$ of the stochastically fluctuating phase turns the equation of motion for $\sigma(t)$ into a multiplicative stochastic differential equation, and the density operator $\sigma(t)$ into a stochastic process. Only the average over many realizations of the process $\phi(t)$ can have relevance, and we write

$$\Pi(t) = \{\sigma(t)\} \tag{9.11}$$

where the brackets $\{...\}$ indicate the average. Then Eq. (9.9) is easily solved for its average, and we obtain the equation of motion for $\Pi(t)$

$$i\frac{d}{dt}\Pi(t) = (L_d - iW - i\Gamma)\Pi(t) \tag{9.12}$$

where the effective relaxation operator, which accounts for the finite laser linewidth, is given by

$$W = \lambda L_g^2 \ . \tag{9.13}$$

This operator can alternatively be represented as

$$W\rho = \lambda(P_g\rho + \rho P_g - 2P_g Tr_a P_g\rho) \tag{9.14}$$

which is reminiscent of the structure of Γ, Eq. (8.6). In Eq. (9.12) we can incorporate the effect of the laser linewidth by the substitution $a_{gg} \rightarrow a_{gg} + 2\lambda$ in the definition of Γ, although in general this is not the correct procedure, as we will see in due course.

X. DRESSED STATES

Both the laser linewidth and the coupling to the phonon reservoir give rise to a damping of the free evolution of the dressed adbond, which is represented by the Liouvillian L_d in Eq. (9.12). This L_d is the analogue of L_a from Eq. (3.17), pertaining to a field-free system. In order to illuminate the physical

picture, we diagonalize the Hamiltonian H_d. First we rewrite Eq. (9.10) as

$$H_d = \sum_{i \neq e,g} \hbar\omega_i P_i + \tfrac{1}{2}\hbar(\omega_e + \omega_g + \omega_L)(P_e + P_g)$$

$$- \tfrac{1}{2}\hbar\Delta(P_e - P_g) - \tfrac{1}{2}\hbar\Omega(|e\rangle\langle g| + |g\rangle\langle e|) \qquad (10.1)$$

with $\Delta = \omega_L - \omega_0$ the detuning from resonance. Diagonalization of H_d is now trivial, and we find the eigenvalue equations to be

$$H_d|k\rangle = \hbar\omega_k|k\rangle \quad , \quad k \neq e,g \qquad (10.2)$$

$$H_d|\pm\rangle = \tfrac{1}{2}\hbar(\omega_e + \omega_g + \omega_L \mp \Omega')|\pm\rangle \qquad (10.3)$$

in terms of the generalized Rabi frequency

$$\Omega' = \Delta(1 + \Omega^2/\Delta^2)^{\tfrac{1}{2}} \quad . \qquad (10.4)$$

Hence the dressed states $|k\rangle$ with $k \neq e,g$ are equal to the adbond states $|k\rangle$, and they have the same eigenvalue, whereas the states $|e\rangle$ and $|g\rangle$ form the linear combination

$$|+\rangle = |g\rangle\sin\tfrac{1}{2}\Theta + |e\rangle\cos\tfrac{1}{2}\Theta \qquad (10.5)$$

$$|-\rangle = |g\rangle\cos\tfrac{1}{2}\Theta - |e\rangle\sin\tfrac{1}{2}\Theta \qquad (10.6)$$

which is parametrized with the angle

$$\Theta = \arctan(\Omega/\Delta). \qquad (10.7)$$

The position of the dressed states with respect to the adbond states is illustrated in Fig. 7.

XI. STEADY STATE

Solving Eq. (9.12) for a transient regime $[0,t]$ has little significance, since a preparation of a specific initial state $\Pi(0)$ is practically not feasible. Any state $\Pi(0)$, however, will relax to the same long-time solution Π on a time scale of the order of Γ^{-1}. Therefore, we consider in some more detail the equation

$$(L_d - iW - i\Gamma)\Pi = 0 \quad . \tag{11.1}$$

Due to the presence of the driving field, the equations for the populations $\Pi_k = \langle k|\Pi|\ell \rangle$ will not necessarily decouple anymore from the equations for the coherences between different states. In general, all matrix elements of $\overline{\Pi}(t)$ couple, but it turns out that in the steady state the coherences for $k \neq \ell$ vanish, provided that $(k,\ell) \neq (e,g)$. Taking matrix elements of Eq. (11.1) shows that the relation between the populations only involves the coherence between the driven transition $|e\rangle - |g\rangle$, as could be expected. Using $\Pi^\dagger = \Pi$ gives the important relation between the real and imaginary parts

$$(A_e + A_g + 2\lambda)\mathrm{Re}\langle e|\Pi|g\rangle = -2\Delta\,\mathrm{Im}\langle e|\Pi|g\rangle \tag{11.2}$$

which enables one to combine the equations for Π_g and Π_e as

$$a_r(\Pi_g - \Pi_e) = \Omega\,\mathrm{Im}\langle e|\Pi|g\rangle \tag{11.3}$$

in terms of the parameter

$$a_r = \tfrac{1}{2}\Omega^2 \frac{\tfrac{1}{2}(A_e + A_g) + \lambda}{\{\tfrac{1}{2}(A_e + A_g) + \lambda\}^2 + \Delta^2} \quad . \tag{11.4}$$

With the aid of Eqs. (11.2) and (11.3) we can eliminate the coherence, which finally yields the set of equations for the populations

$$\sum_\ell \Pi_\ell a_{\ell k} = A_k \Pi_k \quad , \quad k \neq e,g \tag{11.5}$$

$$\sum_{\ell} \Pi_{\ell} a_{\ell e} = A_{e} \Pi_{e} - a_{r}(\Pi_{g} - \Pi_{e}) \tag{11.6}$$

$$\sum_{\ell} \Pi_{\ell} a_{\ell g} = A_{g} \Pi_{g} + a_{r}(\Pi_{g} - \Pi_{e}) \quad . \tag{11.7}$$

This set can be considered as a steady-state analogue of the master equation (8.1).

Inspection of Eqs. (11.5) - (11.7) shows that we can write the set alternatively as

$$\sum_{\ell} \Pi_{\ell} a'_{\ell k} = \sum_{\ell} \Pi_{k} a'_{k\ell} \tag{11.8}$$

where the primed constants are defined as

$$a'_{k\ell} = \begin{cases} a_{k\ell} & , \quad k, \ell \neq e, g \text{ or } g, e \\ \\ a_{k\ell} + a_{r} & , \quad k, \ell = e, g \text{ or } g, e \quad . \end{cases} \tag{11.9}$$

In the same fashion as when we identified the quantity $\Pi_{k} a_{k\ell}$ as the rate of transitions from $|k\rangle$ to $|\ell\rangle$ due to single-phonon processes, we can now interpret $\Pi_{e} a_{r}$ and $\Pi_{g} a_{r}$ as the rates of stimulated radiative transitions from $|e\rangle$ to $|g\rangle$ and from $|g\rangle$ to $|e\rangle$, respectively. We shall see in Section XIV that the optical transitions acquire contributions from both single-photon and multiphoton processes. Notice that the three optical parameters Ω, Δ and λ only enter the equations for the populations through the combination (11.4) in a_{r}. Furthermore, the rate constant a_{r} is linear in the laser power ($\sim \Omega^{2}$), which implies that the number of radiative transitions increases indefinitely with an increasing incident intensity. Obviously, the net absorbed power by a single adsorbed atom should reach a saturation value in the limit of high irradiances. This will be shown in the next section.

XII. LASER HEATING

Radiative excitations of the adbond occur at a rate $a_r \Pi_g$, whereas stimulated emissions of photons in the laser field, accompanied with $|e\rangle \rightarrow |g\rangle$ transitions, happen $a_r \Pi_e$ number of times per unit of time. Balancing the rates gives an effective rate of $a_r(\Pi_g - \Pi_e)$ for the absorption. Every transition corresponds to an effective absorption of a laser photon, so that the power absorption should roughly be equal to $\hbar\omega_L a_r(\Pi_g - \Pi_e)$. Since the accumulated energy in the vibrational bond must be constant in the steady state, the absorbed power from the laser beam equals the power flow into the crystal. This process of laser heating of the substrate is entirely mediated by adsorbates, because the crystal itself was assumed to be transparent.

In Section VI we evaluated the power absorption from a weak monochromatic incident field, by applying the Golden Rule. Obviously, this approach fails for strong, finite linewidth radiation, so that we must find another way to calculate the power absorption. This is accomplished by considering the work done on the dipole moment by the external field, which is formally given by[42]

$$P(t) = \underline{E}(t) \cdot \frac{d}{dt}\langle \underline{\mu}(t)\rangle \quad . \tag{12.1}$$

Here, $\underline{\mu}(t) = \exp(iLt)\underline{\mu}$ and the angle brackets denote the quantum expectation value. Transformation to the Schrödinger picture gives

$$P(t) = \text{Tr}_a[\underline{E}(t) \cdot \underline{\mu}]\frac{d\rho_o}{dt} \tag{12.2}$$

which only involves the reduced density operator $\rho_o(t)$ of the adbond, rather than the Liouvillian L in Eq. (12.1), which pertains to the entire system. With transformation (9.6) we go to the σ-representation, which yields

$$P(t) = \hbar\Omega\{\frac{d}{dt} \text{Re}\langle e|\sigma|g\rangle + (\omega_L + \dot{\phi}(t))\text{Im}\langle e|\sigma|g\rangle\} \quad . \tag{12.3}$$

Application of the equation of motion (9.9) for $\sigma(t)$ results in

$$P(t) = - \tfrac{1}{2}\hbar\Omega(A_e + A_g)\text{Re}\langle e|\sigma|g\rangle + \hbar\Omega\omega_o\text{Im}\langle e|\sigma|g\rangle \qquad (12.4)$$

which elminates both the time derivative and $\dot{\phi}(t)$ from expression (12.3). Equation (12.4) clearly exhibits that power absorption from an external field is reflected in the appearance of coherences in the system.

The quantity $P(t)$ depends stochastically on time, due to the fluctuations in the laser phase. If we define the steady-state power absorption by

$$I(\omega_L) = \lim_{t\to\infty} \{P(t)\} \qquad (12.5)$$

then we obtain $I(\omega_L)$ from Eq. (12.4) with the substitution $\sigma \to \Pi$. Subsequently we use Eqs. (11.2) and (11.3), which amounts to

$$I(\omega_L) = \hbar\{\omega_L - \frac{2\lambda(\omega_L - \omega_o)}{A_e + A_g + 2\lambda}\}a_r(\Pi_g - \Pi_e) . \qquad (12.6)$$

For a monochromatic laser this reduces to $I(\omega_L) = \hbar\omega_L a_r(\Pi_g - \Pi_e)$, as anticipated in the beginning of this section. With increasing laser linewidth λ, the factor in curly brackets tends to ω_o, which reflects that for λ large, the frequency ω_L loses its significance. Then photons are considered to be absorbed in an $|e\rangle \to |g\rangle$ transition, which correponds to an excitation of the sytem with energy $\hbar\omega_o$. Furthermore, we remark that the effect of the laser linewidth in Eq. (12.6) cannot be incorporated by the simple substitution $a_{gg} \to a_{gg} + 2\lambda$, as was the case for the equation of motion for $\Pi(t)$.

With Eq. (11.6) we can cast expression (12.6) in the form

$$I(\omega_L) = \hbar\omega_L'\{A_e\Pi_e - \sum_\ell \Pi_\ell a_{\ell e}\} \qquad (12.7)$$

where ω_L' is an abbreviation for the term in curly brackets in Eq. (12.6).
Representation (12.7) of the power absorption only involves phonon-relaxation
constants, and not a_r anymore. From the restriction $0 \leq \Pi_k \leq 1$, which holds for
every population, we immediately deduce the upper limit

$$I(\omega_L) \leq \hbar\omega_L' A_e \qquad (12.8)$$

for the laser heating of the crystal. Although the rate constant a_r for
stimulated transitions can become arbitrarily large, the net power absorption
exhibits a saturation, where the upper limit is set by the phonon rate constants
rather than by optical parameters. This can be understood from the fact that an
absorbed photon can only be converted into thermal energy through a phonon
transition.

XIII. TRANSITIONS BETWEEN DRESSED STATES

In Section VIII we adopted the secular approximation for the phonon-
transition operator Γ with the argument that the time evolution of $\rho_o(t)$ is
dominated by the free-evolution Liouvillian L_a' of the adbond. This gave rise to
the identification of the rate constants $a_{k\ell}$ for the transitions $|k\rangle \to |\ell\rangle$,
which occur at a rate $n_k(t)a_{k\ell}$. For the strongly-driven adbond, however, the
time evolution of the system is governed by Eq. (9.12) for $\Pi(t)$, which contains
the free evolution of the dressed adbond L_d as the dominant part. Hence it
would seem to be more appropriate to define the secular approximation with
respect to the dressed states, rather than with respect to the field-free
states. Essentially, we should start with Eq. (2.9), include the interaction
$-\underline{\mu}\cdot\underline{E}(t)$ with the laser field in the Hamiltonian, transform to the σ-picture, and
incorporate the phonon coupling. This procedure gives an expression for Γ in
the presence of a driving laser in which we can subsequently drop the non-
secular terms with respect to dressed states. In a previous paper[36] we executed

this laborous scheme, and it turned out that the results are (almost) identical to the simplified derivation which we now give here.

In order to achieve an expression for Γ with respect to dressed states, we merely have to express the projectors P_e and P_g in Eq. (8.6) in dressed-states basis functions $|+\rangle$ and $|-\rangle$. From Eqs. (10.5) and (10.6) we readily find

$$P_e = g_-\hat{P}_+ + g_+\hat{P}_- - g_o(|+\rangle\langle-| + |-\rangle\langle+|) \tag{13.1}$$

$$P_g = g_+\hat{P}_+ + g_-\hat{P}_- + g_o(|+\rangle\langle-| + |-\rangle\langle+|) \tag{13.2}$$

where we have introduced the abbreviations

$$g_- = \cos^2\tfrac{1}{2}\Theta \quad , \quad g_+ = \sin^2\tfrac{1}{2}\Theta \quad , \quad g_o = \cos\tfrac{1}{2}\Theta\sin\tfrac{1}{2}\Theta \quad , \tag{13.3}$$

and the projectors $\hat{P}_\pm = |\pm\rangle\langle\pm|$ onto the dressed states. Next we substitute the expansions (13.1) and (13.2) into Eq. (8.6), and drop the non-secular terms. Care should be exercised, however, because a $|+\rangle \rightarrow |+\rangle$ transition between two doublets (Fig.7) is in exact resonance with a $|-\rangle \rightarrow |-\rangle$ transition, and therefore couplings between these transitions should be retained. Combining everything then results in

$$\Gamma\rho = \tfrac{1}{2} \sum_{k\ell} \hat{a}_{k\ell}(\hat{P}_k\rho + \rho\hat{P}_k - 2\hat{P}_\ell Tr_a\hat{P}_k\rho)$$

$$+ g_o^2(a_{eg} - a_{ee} + a_{ge} - a_{gg})(\hat{P}_+\rho\hat{P}_- + \hat{P}_-\rho\hat{P}_+) \tag{13.4}$$

where the term proportional to g_o^2 comes from the mentioned degeneracy, and $\hat{P}_k$ denotes a projector onto a dressed state. Representation (13.4) gives rise to a master equation with respect to dressed states, which implies that we can interpret the parameters $\hat{a}_{k\ell}$ as the rate constants for transitions between dressed states.

Of course, the parameters $\hat{a}_{k\ell}$ can be related to the relaxation constants $a_{k\ell}$ with respect to the adbond states. For $k \neq e,g$ and $\ell \neq e,g$, we obviously have $\hat{a}_{k\ell} = a_{k\ell}$. If one of the states $|k\rangle$, $|\ell\rangle$ equals a $|+\rangle$ or $|-\rangle$ state, we find

$$\hat{a}_{k\pm} = g_{\mp} a_{ke} + g_{\pm} a_{kg} \tag{13.5}$$

$$\hat{a}_{\pm k} = g_{\mp} a_{ek} + g_{\pm} a_{gk} \tag{13.6}$$

in terms of the optical parameters $g_{\pm}$. Transitions between the $|+\rangle$ and $|-\rangle$ states are governed by the rate constants

$$\hat{a}_{\pm\mp} = g_{\pm}^2 a_{ge} + g_{\mp}^2 a_{eg} + g_o^2 (a_{ee} + a_{gg}) \tag{13.7}$$

$$\hat{a}_{\pm\pm} = g_o^2 (a_{ge} + a_{eg}) + g_{\mp}^2 a_{ee} + g_{\pm}^2 a_{gg} \ . \tag{13.8}$$

Interaction with the phonon field is now regarded as the occurrence of single-phonon transitions between dressed states. Relaxation constants which connect an adbond state $|k\rangle \neq |e\rangle$ or $|g\rangle$ with a dressed state $|+\rangle$ or $|-\rangle$ acquire a contribution from two distinct processes, due to the fact that $|k\rangle$ couples with both the doublets in Fig. 7. In order to find out which term corresponds to which transition, we recall the definition (7.5) of the parameter $a_{k\ell}$. We notice that the reservoir correlation function $\tilde{G}$ is evaluated at $\Delta_{k\ell}$, which equals the frequency of the phonon for that particular transition. Therefore, the terms with a_{ek} and a_{ke} represent transitions from and to the upper doublet, respectively, whereas the terms with a_{gk}, a_{kg} describe single-phonon transitions between $|k\rangle$ and the lower states. In a similar way we can interpret the various terms in Eqs. (13.7) and (13.8). In Fig. 8 the different processes are indicated by arrows, and the accompanying optical factor specifies the term in Eqs. (13.5) - (13.8).

XIV.   PHOTON-PHONON CONVERSION

Stimulated radiative transitions between adbond states are incorporated in the diagonalization of $H_a - \underline{\mu} \cdot \underline{E}$, and therefore only single-phonon transitions persist in a pictorial representation of the various processes with respect to the dressed states.   In order to elucidate the mechanism of photon absorption, and to establish the relation with the process of laser heating, we consider the limit of (relatively) low laser power.   To this end, we first note that $g_{\pm}$ can be expressed in Ω and Δ according to

$$g_{\pm} = \tfrac{1}{2}\{1 \mp (1 + \Omega^2/\Delta^2)^{-\frac{1}{2}}\} \qquad (14.1)$$

which depends only on the optical parameters through the combination Ω^2/Δ^2.   For weak fields we then obtain

$$g_{-} \simeq 1 - \Omega^2/4\Delta^2 \quad , \quad g_{+} \simeq \Omega^2/4\Delta^2 \qquad (14.2)$$

which shows that g_{-} remains present without a radiation field.   Rate constants which are proportional to g_{-} must consequently correspond to radiationless transitions.   On the other hand, the factor g_{+} is proportional to the laser power, which implies that every factor g_{+} in a $\hat{a}_{k\ell}$ corresponds to the absorption or emission of a photon.   In this fashion we can track down the significance of the optical factors in the relaxation constants with respect to dressed states. In Fig. 9 we draw the diagrams with respect to the adbond states, and they are in the same order as the corresponding diagrams of Fig. 8.   All transitions with a rate constant proportional to $g_o^2 = g_{-} g_{+}$ are single-photon processes.

Now it should be obvious how the process of laser heating of the crystal can be conceived as a result of many photon-phonon conversion reactions.   Every phonon in the diagram corresponds to an energy exchange between the adbond and the crystal, whereas a photon transition amounts to an energy transfer between

the laser field and the adbond. A combined photon-phonon diagram, therefore, represent effectively an exchange of energy between the laser and the crystal, a process which is mediated by the adsorbate. Summation of the contributions from all diagrams, weighted with the probabilities for the diagrams to occur, then gives the net power absorption by the crystal.

XV. SUMMARY

We have studied theoretically the optical properties of an adsorbed atom, in a vibrational bond, on a crystal. Coupling of the adbond states with the phonon field of the substrate have been assumed to be brought about by single-phonon transitions only, which is the main approximation in the presented theory. It is straightforward, however, to include higher-order processes, especially when the interaction is taken to be a Morse potential. Then all matrix elements can be evaluated analytically, and a system with an arbitrary number of adbond states can be parametrized with the depth, width and position of the binding potential. We have chosen to restrict the approach to single-phonon transitions, which allows a clear interpretation of the coupling mechanism. Then we can incorporate the interaction with the crystal with a single phonon-field amplitude correlation function $G(\tau)$, which was studied in detail in Section IV. It is the behavior of this crystal-response function that determines whether the reservoir approach to thermal relaxation can be justified or not. In particular, the decay of $G(\tau)$ must be sufficiently fast, in comparison with the adbond relaxation rates, in order to impose a Markovian time evolution on the reduced adbond density-operator. This decay time is typically of the order of the inverse Debye frequency, which is reasonably small in comparison with the rate constants for a single-phonon process (~ one order of magnitude).

Subsequently, the absorption line shape has been evaluated, showing considerable deviation from a Lorentzian in certain cases. The origin of the distortions and the shifts, other than the common Lamb shift, has been tracked down to the presence of non-secular terms in the time evolution of the density operator, which in turn appears as a consequence of the fact that the damping constants are not necessarily small in comparison with the transition frequencies.

Next, we have considered the irradiation of the adsorbate by an intense non-monochromatic laser. The laser linewidth is assumed to arise from a stochastically-fluctuating diffusive phase of the driving field. Diagonialization of the Hamiltonian is accomplished by a stochastic transformation, which yields the dressed states. These states can be interpreted as the joint eigenstates of the adbond, the single-mode laser and their interaction. We have analyzed the equation of motion for this sytem and discussed some properties of the steady state. In particular, the coherence of the driven transition does not disappear in the long-time limit, which indicates that the system is not in thermal equilibrium.

Then the power absorption has been obtained from the work done on the dipole by the external field. The finite bandwidth of the laser gives rise to an effective photon energy $\hbar\omega_L'$, with ω_L' in between ω_0 and ω_L. Then the power absorption can be written as $I(\omega_L) = \hbar\omega_L' a_r (\Pi_g - \Pi_e)$, with a_r the rate of optical transitions. It has been shown that a_r is linear in the laser intensity, which implies that $\Pi_g - \Pi_e$ tends to zero in the high-intensity limit, since the absorption rate must remain finite. Stimulated transitions, which occur at a rate a_r, Eq. (11.4), are reduced by an increasing linewidth, if the system is driven close to resonance ($\Delta \simeq 0$), whereas far off resonance the linewidth enhances the number of transitions ($a_r \sim \lambda$). This feature is easily understood:

in the case $\Delta \sim 0$ most laser photons are farther off resonance than for monochromatic incident radiation. On the other hand, for a large detuning there is still a considerable amount of photons in close resonance, which have a large probability to be absorbed.

As a last issue, we have derived the rate constants for single-phonon transitions between dressed states. In the low-intensity limit, these processes can be interpreted as single-phonon/multiphoton processes in adbond-state diagrams, where "multi" stands for zero, one or two. This reveals that photoabsorption is inevitably accompanied by a downward phonon transition, which gives rise to heating of the crystal. Light-induced desorption through resonant excitation of a high-lying state is consequently bound to have an extremely low efficiency.

ACKNOWLEDGMENTS

REFERENCES

1. G. Nienhuis, Physica 66, 245 (1973).

2. R. B. Hall and S. J. Bares, in Chemistry and Structure at Interfaces, edited by R. B. Hall and A. B. Elles (VCH publishers, Deerfield Beach, Florida, 1986) pp. 83-149.

3. E. J. Heilweil, M. P. Casassa, R. R. Cavanagh and J. C. Stephenson, J. Chem. Phys. 82, 5216 (1985).

4. S. Chiang, R. G. Tobin, P. L. Richards and P. A. Thiel, Phys. Rev. Lett. 52, 648 (1984).

5. M. S. Djidjoev, R. V. Khokhlov, A. V. Kiselev, V. I. Lygin, V. A. Namiot, A. I. Osipov, V. I. Puchenko and B. I. Provotorov, in Tunable Lasers and Applications, edited by A. Mooradian, T. Jaeger and P. Stokseth (Springer, Berlin, 1976), pp. 100-107.

6. M. S. Slutsky and T. F. George, Chem. Phys. Lett. 57, 474 (1978).

7. M. S. Slutsky and T. F. George, J. Chem. Phys. 70, 1231 (1979).

8. J. Heidberg, H. Stein and E. Riehl, Phys. Rev. Lett. 49, 666 (1982).

9. T. J. Chuang, J. Chem. Phys. 76, 3828 (1982).

10. T. J. Chuang and H. Seki, Phys. Rev. Lett. 49, 382 (1982).

11. J. Heidberg and I. Hussla, J. Electron. Spectrosc. Rel. Phen. 29, 105 (1983).

12. I. Hussla, H. Seki, T. J. Chuang, Z. W. Gortel, H. J. Kreuzer and P. Piercy, Phys. Rev. B. 32, 3489 (1985).

13. K. Veeken, P. A. M. van der Heide, L. M. ten Dam, A. R. de Vroomen and J. Reuss, Surf. Sci. 166, 1 (1986).

14. T. J. Chuang, Surf. Sci. Rep. 3, 1 (1983).

15. Z. W. Gortel, H. J. Kreuzer and R. Teshima, Phys. Rev. B 22, 5655 (1980).

16. S. Efrima, K. F. Freed, C. Jedrzejek and H. Metiu, Chem. Phys. Lett. 74, 43 (1980).

17. C. Jedrzejek, K. F. Freed, S. Efrima and H. Metiu, Chem. Phys. Lett. 79, 227 (1981).

18. Z. W. Gortel, H. J. Kreuzer, R. Teshima and L. A. Turski, Phys. Rev. B 24, 4456 (1981).

19. S. Efrima, C. Jedrzejek, K. F. Freed, E. Hood and H. Metiu, J. Chem. Phys. 79, 2436 (1983).

20. B. J. Garrison, D. J. Diestler and S. A. Adelman, J. Chem. Phys. $\underline{67}$, 4317 (1977).

21. A. A. Maradudin, E. W. Montroll, G. H. Weiss and I. P. Ipatova, Theory of Lattice Dynamics in the Harmonic Approximation, Solid State Physics, 2nd Ed. Suppl. 3 (Academic Press, New York, 1971).

22. R. W. Zwanzig, in Lectures in Theoretical Physics, Vol. III, edited by W. E. Britten, B. Downs and J. Downs (Interscience, New York, 1961), p. 106 ff.

23. W. H. Louisell, Quantum Statistical Properties of Radiation (Wiley, New York, 1973), Ch. 6.

24. C. Cohen-Tannoudji, in Frontiers in Laser Spectroscopy, Proc. 27th Les Houches Summer School, edited by R. Balian, S. Haroche and S. Liberman (North-Holland, Amsterdam, 1977).

25. S. van Smaalen and T. F. George, Phys. Rev. B, submitted.

26. A. Ben-Reuven, Adv. Chem. Phys. $\underline{33}$, 235 (1975).

27. M. Lax, Phys. Rev. $\underline{172}$, 350 (1968).

28. G. Korzeniewski, E. Hood and H. Metiu, J. Vac. Sci. Technol. $\underline{20}$, 594 (1982).

29. J. Lin, X. Y. Huang and T. F. George, Z. Phys. B $\underline{48}$, 355 (1982).

30. Z. W. Gortel, H. J. Kreuzer, P. Piercy and R. Teshima, Phys. Rev. B $\underline{27}$, 5066 (1983).

31. X. Y. Huang, T. F. George and J. M. Yuan, J. Opt. Soc. Am. B $\underline{2}$, 985 (1985).

32. B. Fain and S. H. Lin, Physica $\underline{138}$ B, 63 (1986).

33. J. Lin and T. F. George, J. Phys. Chem. $\underline{84}$, 2957 (1980).

34. J. Lin, X. Y. Huang and T. F. George, J. Vac. Sci. Technol. B $\underline{3}$, 1525 (1985).

35. A. C. Beri and T. F. George, J. Vac. Sci. Technol. B $\underline{3}$, 1529 (1985).

36. H. F. Arnoldus, S. van Smaalen and T. F. George, Phys. Rev. B $\underline{34}$, 6902 (1986).

37. S. van Smaalen, H. F. Arnoldus and T. F. George, Phys. Rev. B (1986) in press.

38. H. F. Arnoldus and T. F. George, J. Opt. Soc. Am. B (1987) in press.

39. H. F. Arnoldus and G. Nienhuis, J. Phys. B: At. Mol. Phys. $\underline{19}$, 873 (1986).

40. N. G. van Kampen, Stochastic Processes in Physics and Chemistry (North-Holland, Amsterdam, 1981).

41. H. F. Arnoldus and G. Nienhuis, J. Phys. B: At. Mol. Phys. $\underline{16}$, 2325 (1983).

42. L. Allen and J. H. Eberly, Optical Resonance and Two-Level Atoms (Wiley, New York, 1975).

43. G. S. Agarwal, Phys. Rev. A $\underline{18}$, 1490 (1978).

FIGURE CAPTIONS

Fig. 1. Real (a) and imaginary (b) parts of the correlation function $G(\tau)_{sp}$, divided by $\frac{1}{2}\zeta\omega_D^{-1}$, and as a function of $\omega_D\tau$. From Eq. (4.11) it follows that the integral over curve (a) equals zero.

Fig. 2. Stimulated part of the reservoir correlation function, divided by $2\zeta\omega_D^{-2}kT/\hbar$, and as a function of $\omega_D\tau$. Curve (a) corresponds to $\hbar\omega_D = 0.001kT$ (high-temperature limit), and for curve (b) we have taken $\hbar\omega_D = 4kT$ (low-temperature region).

Fig. 3. Real (a) and imaginary (b) parts of the Fourier-Laplace transform of the spontaneous part of the correlation function, divided by $\zeta\omega_D^{-2}$, and as a function of ω/ω_D. The real part vanishes for $\omega < 0$ and for $\omega > \omega_D$, whereas an imaginary part is present for every ω.

Fig. 4. Same as Fig. 3, but now for the stimulated part. Normalized by $\zeta kT/\hbar\omega_D^3$ and for $\hbar\omega_D = 3kT$. The real part only vanishes for $|\omega| > \omega_D$. Singularities in the imaginary part appear at $\omega = \pm\omega_D$, which is an artefact of the sharp cut-off of the dispersion relation at ω_D. Any smooth decay for $\omega > \omega_D$, but still arbitrarily steep, will result in a finite value of the correlation function at $\omega = \pm\omega_D$.

Fig. 5. Absorption line as a function of ω_L, and divided by $I_L B(\bar{n}_1 - \bar{n}_2)\hbar$. Frequencies are in units of ω_o. The parameters for these curves are $\mathrm{Im}\eta = 0$ and $\mathrm{Re}\eta = 0.5, 1, 2$ for a,b,c, respectively. For a decreasing $\mathrm{Re}\eta$ (~ linewidth), the profile tends to a Lorentzian with half-width at half-maximum equal to $\mathrm{Re}\eta$. For $\mathrm{Im}\eta = 0$ the maximum is always situated at $\omega_L = \omega_o$.

Fig. 6. Same as Fig. 5 but now with $\mathrm{Re}\eta = 0.2$ for all three curves. The imaginary parts of η, the lamb shift, are +0.3, -0.5 and -0.6 for a, b and c respectively. For $\mathrm{Im}\eta$ small, the line around $\omega_L = \omega_o$ only shifts over a distance $\mathrm{Im}\eta$, but for larger values the line shape changes dramatically. The

top of the curve is always at $\omega_L = \omega_o(|1+2\text{Im}\eta/\omega_o|)^{\frac{1}{2}}$, which is independent of Reη. For Imη small in comparison with ω_o the top appears to $\omega_L \simeq \omega_o + \text{Im}\eta$.

Fig. 7. Diagonalization of the dressed-adbond Hamiltonian. The diagram on the left-hand side represent product states of the adbond $|e\rangle, |g\rangle, |k\rangle, \ldots$ and the free evolving laser $|n\rangle$, with $n = 0,1,2\ldots$ the number of photons in the mode. States $|n\rangle$ and $|n+1\rangle$ are separated by the photon frequency ω_L. In this diagram we have taken $\Delta = \omega_L - \omega_o > 0$. Since the laser is assumed to be almost on resonance, we have a ladder of doublets separated by the detuning Δ. Then the dipole interaction couples the states which form a doublet, but it does not couple two sets of states. A diagonalization in turn gives rise to the diagram on the right-hand side, where the separation in the new doublets equals Ω', which is always larger than Δ.
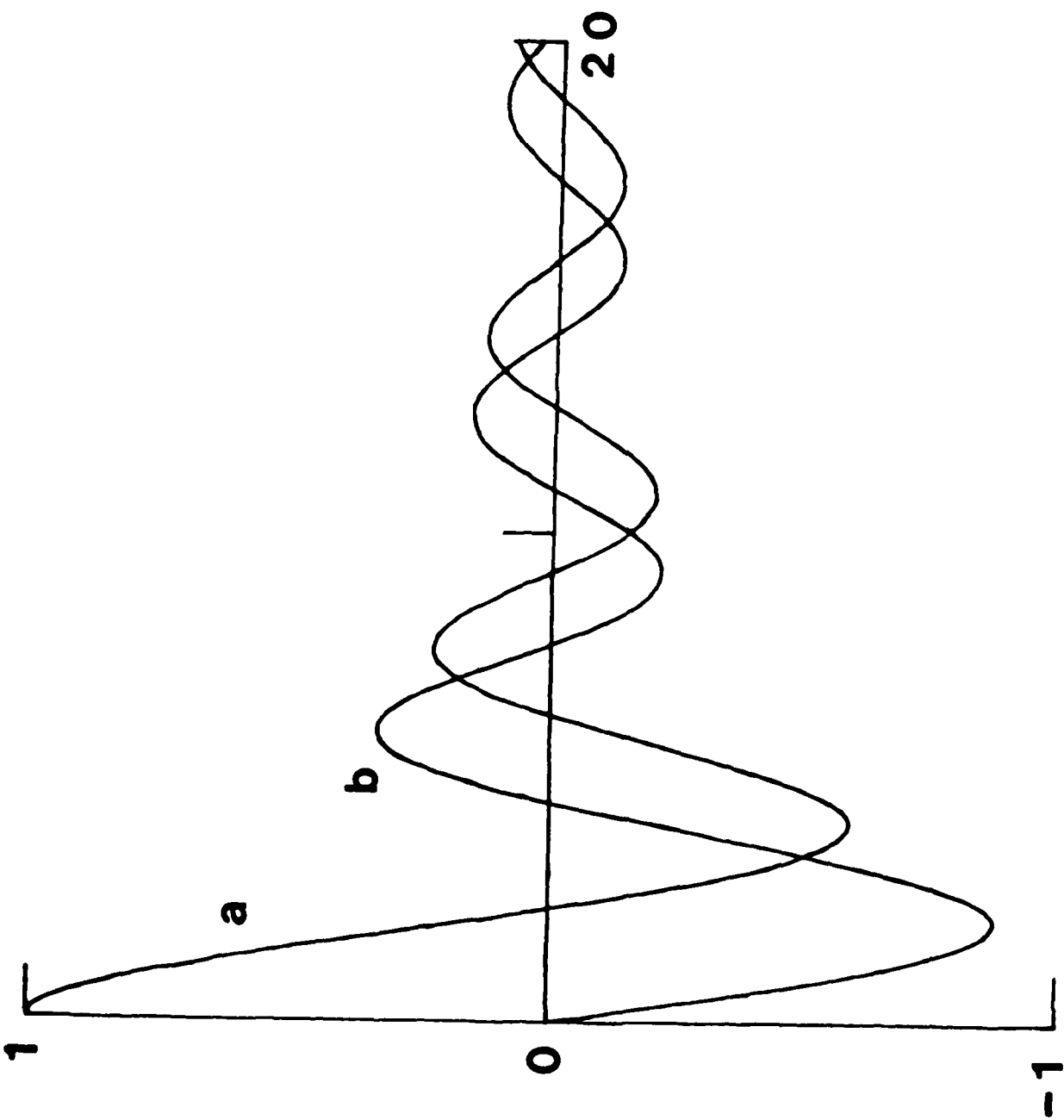
Fig. 8. Single-phonon excitations of the laser-adbond system. The diagrams with the arrows in the opposite direction (not shown here) correspond to phonon emission into the crystal. The three diagrams with the double arrows persist in the absence of the laser and correspond to radiationless transitions between adbond states. Solid arrows have rate constants proportional to g_+, so that they represent single-photon processes. For strong fields the g_+^2 transition appears, which couples the two doublets by a two-photon process. The right-most diagrams give transitions in a single doublet via a single-photon process. Their rate costants are proportional to the diagonal matrix elements of the derivative of the binding potential, which are small. For zero temperature these transitions vanish identically, since then we have $a_{ee} = a_{gg} = 0$.
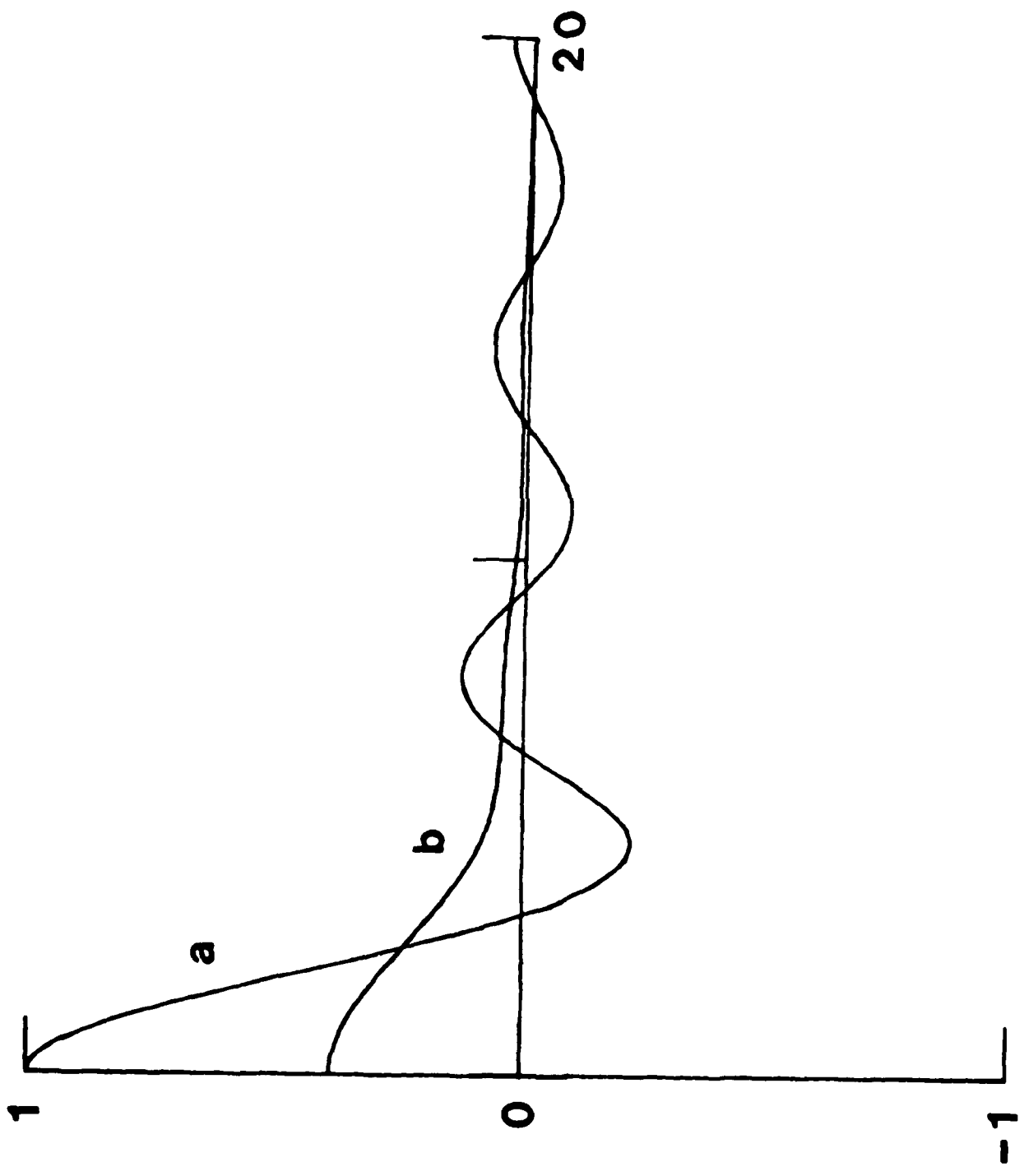
Fig. 9. Low-intensity interpretation of the diagrams from Fig. 8. With respect to the adbond states, a single-phonon process goes together with photon absorptions and emissions in such a way that the resulting diagram is energy conserving. The sequence of processes in a single diagram can only give rise to
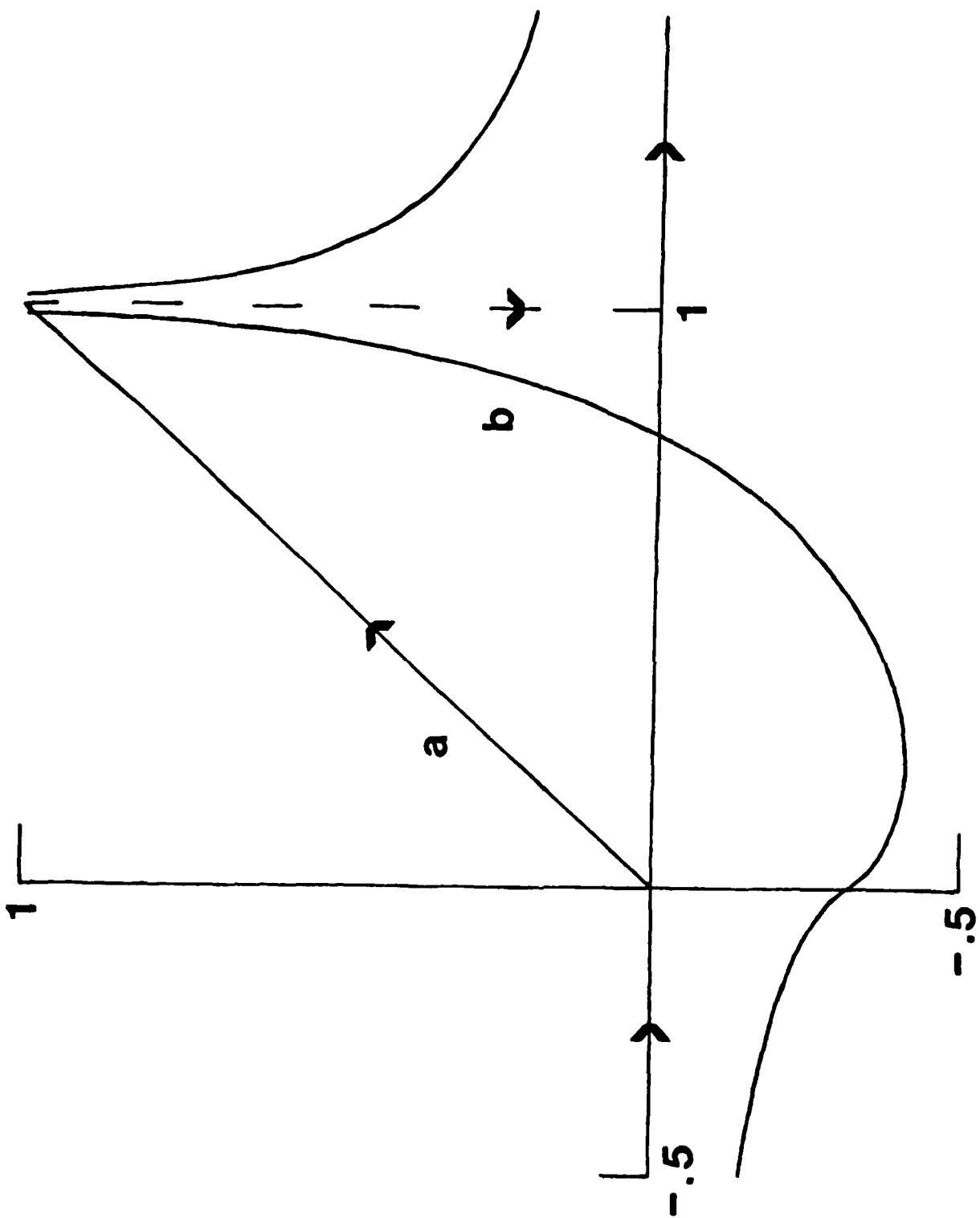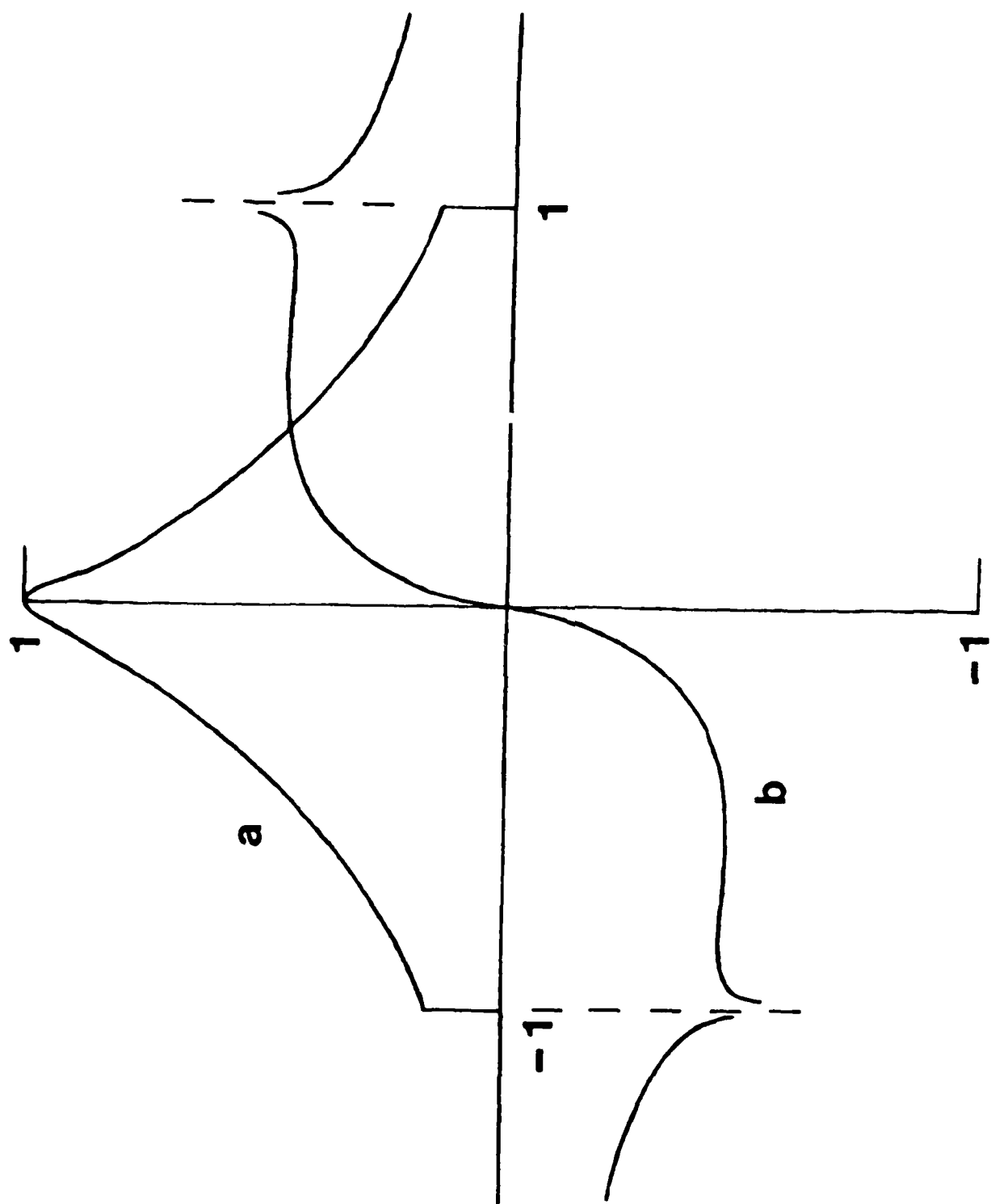
transitions between the real states $|e\rangle, |g\rangle, |k\rangle, \ldots$, but intermediate states can be virtual in this picture. The diagrams are in the same order as in Fig. 8, and for the phonon-emission processes we simply reverse the directions of all arrows.
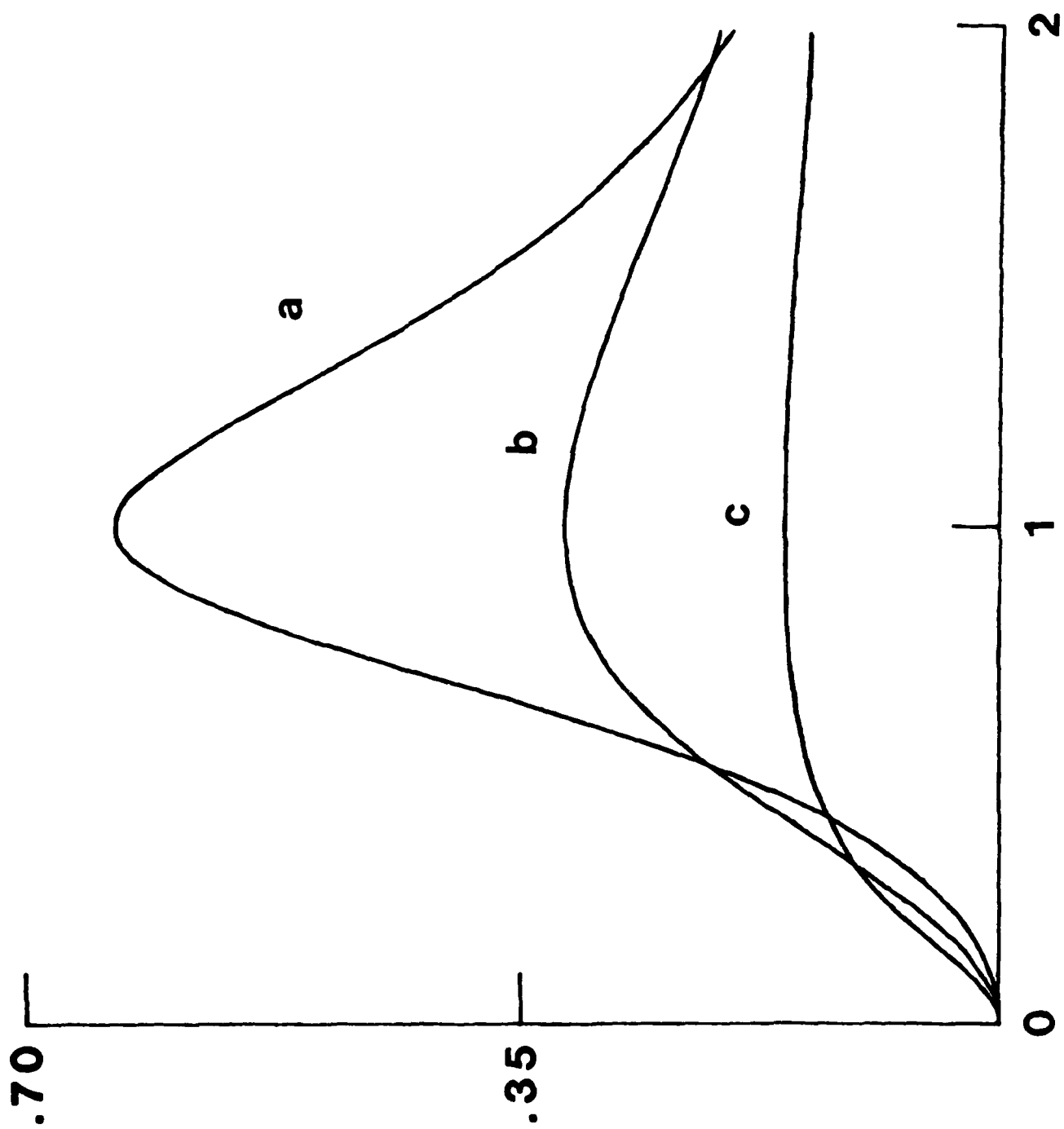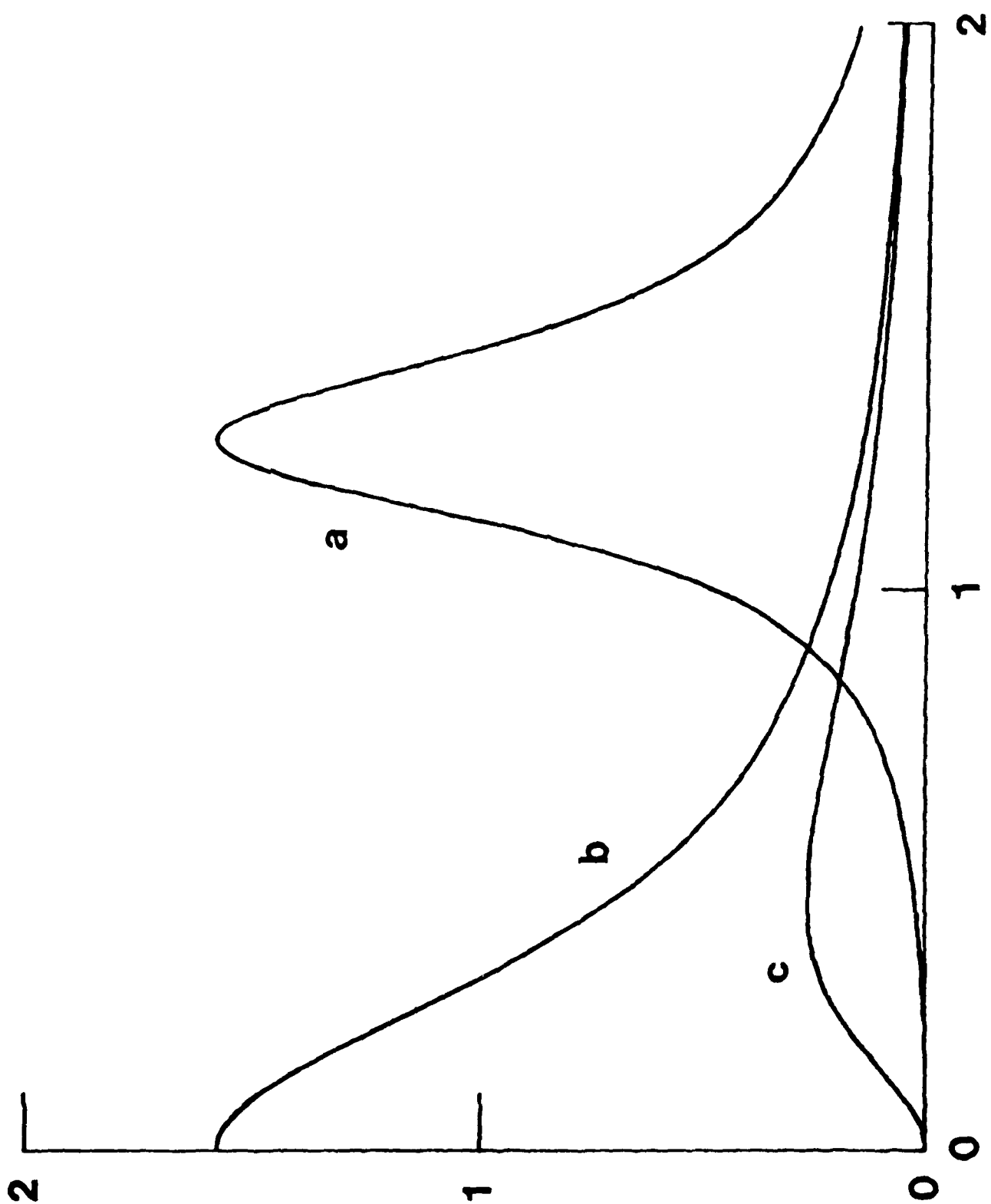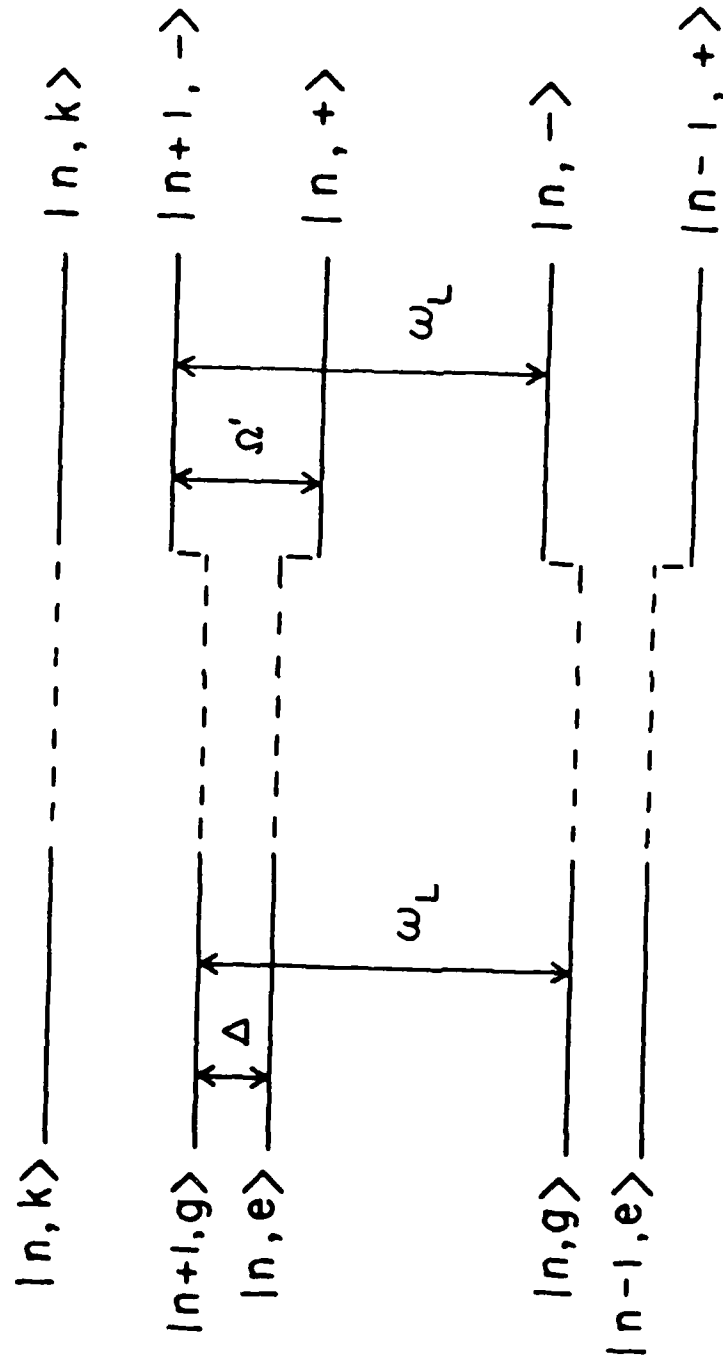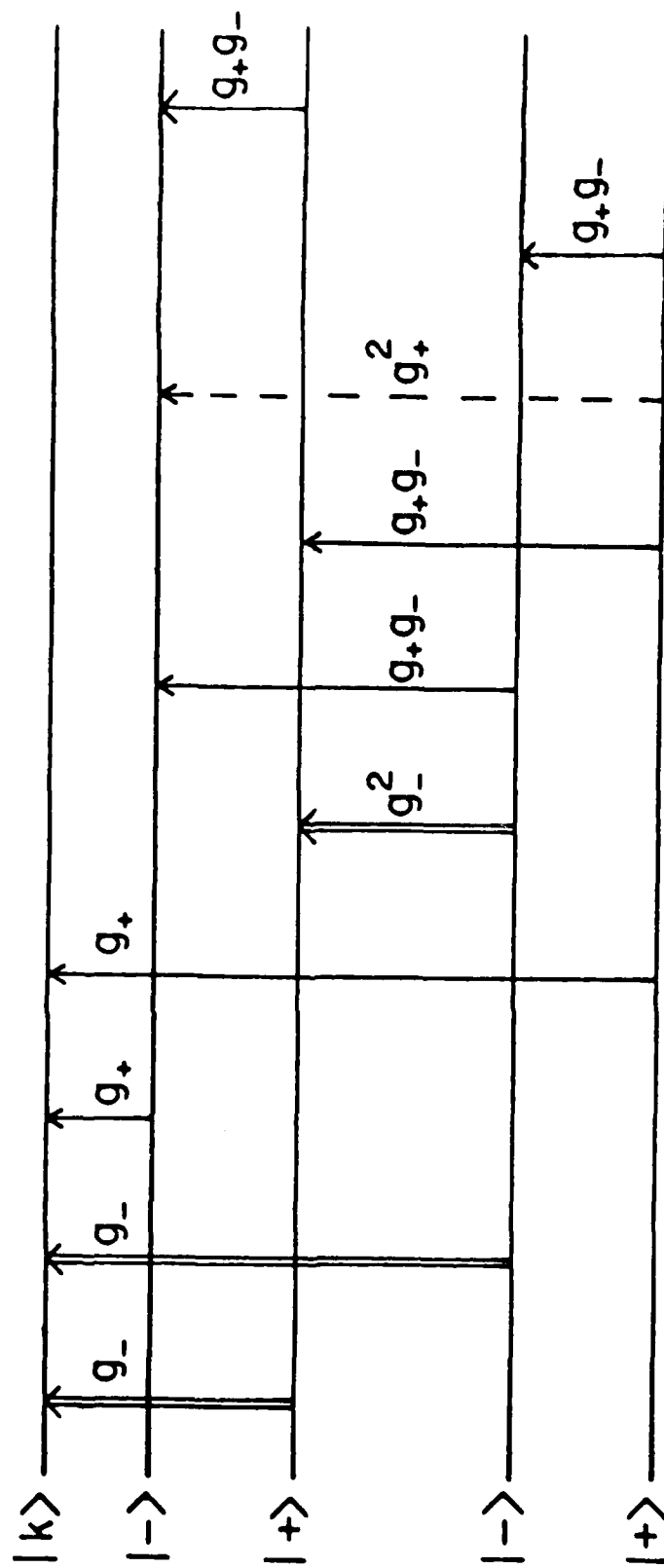
Fig. 7

$|k\rangle$

$|-\rangle$

$|+\rangle$

$|-\rangle$

$|+\rangle$

g_-

g_-

g_+

g_+

g_-^2

g_+g_-

g_+g_-

$|g_+^2$

g_+g_-

g_+g_-

$|k\rangle$

$|e\rangle$

Δ

$|g\rangle$

Δ
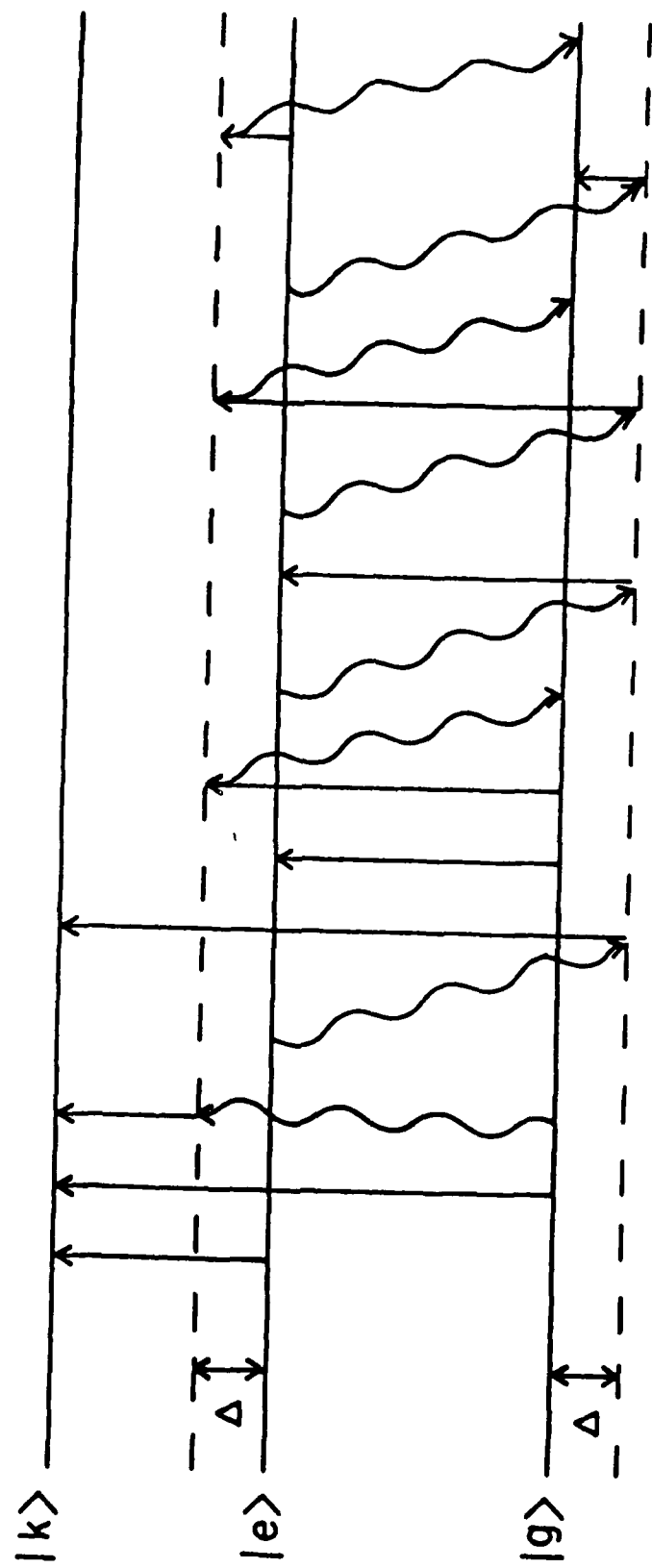
TECHNICAL REPORT DISTRIBUTION LIST, GEN

	No. Copies		No. Copies
Office of Naval Research Attn: Code 1113 800 N. Quincy Street Arlington, Virginia 22217-5000	2	Dr. David Young Code 334 NORDA NSTL, Mississippi 39529	1
Dr. Bernard Douda Naval Weapons Support Center Code 50C Crane, Indiana 47522-5050	1	Naval Weapons Center Attn: Dr. Ron Atkins Chemistry Division China Lake, California 93555	1
Naval Civil Engineering Laboratory Attn: Dr. R. W. Drisko, Code L52 Port Hueneme, California 93401	1	Scientific Advisor Commandant of the Marine Corps Code RD-1 Washington, D.C. 20380	1
Defense Technical Information Center Building 5, Cameron Station Alexandria, Virginia 22314	12 high quality	U.S. Army Research Office Attn: CRD-AA-IP P.O. Box 12211 Research Triangle Park, NC 27709	1
DTNSRDC Attn: Dr. H. Singerman Applied Chemistry Division Annapolis, Maryland 21401	1	Mr. John Boyle Materials Branch Naval Ship Engineering Center Philadelphia, Pennsylvania 19112	1
Dr. William Tolles Superintendent Chemistry Division, Code 6100 Naval Research Laboratory Washington, D.C. 20375-5000	1	Naval Ocean Systems Center Attn: Dr. S. Yamamoto Marine Sciences Division San Diego, California 91232	1
		Dr. David L. Nelson Chemistry Division Office of Naval Research 800 North Quincy Street Arlington, Virginia 22217	1

ABSTRACTS DISTRIBUTION LIST, 056/625/629

Dr. J. E. Jensen
Hughes Research Laboratory
3011 Malibu Canyon Road
Malibu, California 90265

Dr. J. H. Weaver
Department of Chemical Engineering
  and Materials Science
University of Minnesota
Minneapolis, Minnesota 55455

Dr. A. Reisman
Microelectronics Center of North Carolina
Research Triangle Park, North Carolina
    27709

Dr. M. Grunze
Laboratory for Surface Science and
        Technology
University of Maine
Orono, Maine 04469

Dr. J. Butler
Naval Research Laboratory
Code 6115
Washington D.C. 20375-5000

Dr. L. Interante
Chemistry Department
Rensselaer Polytechnic Institute
Troy, New York 12181

Dr. Irvin Heard
Chemistry and Physics Department
Lincoln University
Lincoln University, Pennsylvania 19352

Dr. K.J. Klaubunde
Department of Chemistry
Kansas State University
Manhattan, Kansas 66506

Dr. C. B. Harris
Department of Chemistry
University of California
Berkeley, California 94720

Dr. F. Kutzler
Department of Chemistry
Box 5055
Tennessee Technological University
Cookesville, Tennessee 38501

Dr. D. DiLella
Chemistry Department
George Washington University
Washington D.C. 20052

Dr. R. Reeves
Chemistry Department
Renssaeler Polytechnic Institute
Troy, New York 12181

Dr. Steven M. George
Stanford University
Department of Chemistry
Stanford, CA 94305

Dr. Mark Johnson
Yale University
Department of Chemistry
New Haven, CT 06511-8118

Dr. W. Knauer
Hughes Research Laboratory
3011 Malibu Canyon Road
Malibu, California 90265

6

ABSTRACTS DISTRIBUTION LIST, 056/625/629

Dr. G. A. Somorjai
Department of Chemistry
University of California
Berkeley, California 94720

Dr. J. Murday
Naval Research Laboratory
Code 6170
Washington, D.C. 20375-5000

Dr. J. B. Hudson
Materials Division
Rensselaer Polytechnic Institute
Troy, New York 12181

Dr. Theodore E. Madey
Surface Chemistry Section
Department of Commerce
National Bureau of Standards
Washington, D.C. 20234

Dr. J. E. Demuth
IBM Corporation
Thomas J. Watson Research Center
P.O. Box 218
Yorktown Heights, New York 10598

Dr. M. G. Lagally
Department of Metallurgical
  and Mining Engineering
University of Wisconsin
Madison, Wisconsin 53706

Dr. R. P. Van Duyne
Chemistry Department
Northwestern University
Evanston, Illinois 60637

Dr. J. M. White
Department of Chemistry
University of Texas
Austin, Texas 78712

Dr. D. E. Harrison
Department of Physics
Naval Postgraduate School
Monterey, California 93940

Dr. R. L. Park
Director, Center of Materials
  Research
University of Maryland
College Park, Maryland 20742

Dr. W. T. Peria
Electrical Engineering Department
University of Minnesota
Minneapolis, Minnesota 55455

Dr. Keith H. Johnson
Department of Metallurgy and
  Materials Science
Massachusetts Institute of Technology
Cambridge, Massachusetts 02139

Dr. S. Sibener
Department of Chemistry
James Franck Institute
5640 Ellis Avenue
Chicago, Illinois 60637

Dr. Arnold Green
Quantum Surface Dynamics Branch
Code 3817
Naval Weapons Center
China Lake, California 93555

Dr. A. Wold
Department of Chemistry
Brown University
Providence, Rhode Island 02912

Dr. S. L. Bernasek
Department of Chemistry
Princeton University
Princeton, New Jersey 08544

Dr. W. Kohn
Department of Physics
University of California, San Diego
La Jolla, California 92037

7

ABSTRACTS DISTRIBUTION LIST, 056/625/629

Dr. F. Carter
Code 6170
Naval Research Laboratory
Washington, D.C. 20375-5000

Dr. Richard Colton
Code 6170
Naval Research Laboratory
Washington, D.C. 20375-5000

Dr. Dan Pierce
National Bureau of Standards
Optical Physics Division
Washington, D.C. 20234

Dr. R. Stanley Williams
Department of Chemistry
University of California
Los Angeles, California 90024

Dr. R. P. Messmer
Materials Characterization Lab.
General Electric Company
Schenectady, New York 22217

Dr. Robert Gomer
Department of Chemistry
James Franck Institute
5640 Ellis Avenue
Chicago, Illinois 60637

Dr. Ronald Lee
R301
Naval Surface Weapons Center
White Oak
Silver Spring, Maryland 20910

Dr. Paul Schoen
Code 6190
Naval Research Laboratory
Washington, D.C. 20375-5000

Dr. John T. Yates
Department of Chemistry
University of Pittsburgh
Pittsburgh, Pennsylvania 15260

Dr. Richard Greene
Code 5230
Naval Research Laboratory
Washington, D.C. 20375-5000

Dr. L. Kesmodel
Department of Physics
Indiana University
Bloomington, Indiana 47403

Dr. K. C. Janda
University of Pittsburg
Chemistry Building
Pittsburg, PA 15260

Dr. E. A. Irene
Department of Chemistry
University of North Carolina
Chapel Hill, North Carolina 27514

Dr. Adam Heller
Bell Laboratories
Murray Hill, New Jersey 07974

Dr. Martin Fleischmann
Department of Chemistry
University of Southampton
Southampton 509 5NH
UNITED KINGDOM

Dr. H. Tachikawa
Chemistry Department
Jackson State University
Jackson, Mississippi 39217

Dr. John W. Wilkins
Cornell University
Laboratory of Atomic and
  Solid State Physics
Ithaca, New York 14853

ABSTRACTS DISTRIBUTION LIST, 056/625/629

Dr. R. G. Wallis
Department of Physics
University of California
Irvine, California 92664

Dr. D. Ramaker
Chemistry Department
George Washington University
Washington, D.C. 20052

Dr. J. C. Hemminger   .
Chemistry Department
University of California
Irvine, California 92717

Dr. T. F. George
Chemistry Department
University of Rochester
Rochester, New York 14627

Dr. G. Rubloff
IBM
Thomas J. Watson Research Center
P.O. Box 218
Yorktown Heights, New York 10598

Dr. Horia Metiu
Chemistry Department
University of California
Santa Barbara, California 93106

Dr. W. Goddard
Department of Chemistry and Chemical
    Engineering
California Institute of Technology
Pasadena, California 91125

Dr. P. Hansma
Department of Physics
University of California
Santa Barbara, California 93106

Dr. J. Baldeschwieler
Department of Chemistry and
   Chemical Engineering
California Institute of Technology
Pasadena, California 91125

Dr. J. T. Keiser
Department of Chemistry
University of Richmond
Richmond, Virginia 23173

Dr. R. W. Plummer
Department of Physics
University of Pennsylvania
Philadelphia, Pennsylvania 19104

Dr. E. Yeager
Department of Chemistry
Case Western Reserve University
Cleveland, Ohio 41106

Dr. N. Winograd
Department of Chemistry
Pennsylvania State University
University Park, Pennsylvania 16802

Dr. Roald Hoffmann
Department of Chemistry
Cornell University
Ithaca, New York 14853

Dr. A. Steckl
Department of Electrical and
    Systems Engineering
Rensselaer Polytechnic Institute
Troy, NewYork 12181

Dr. G.H. Morrison
Department of Chemistry
Cornell University
Ithaca, New York 14853

END

2-87

DTIC